SECOND ANNUAL REPORT

on

END POINT CONTROL OF FLEXIBLE ROBOTS

at

STANFORD UNIVERSITY

with major funding from

DEFENSE ADVANCED RESEARCH PROJECTS ADMINISTRATION

Contract No: F33615-82-K-5108

Principal Investigators:

Professor Thomas O. Binford

Professor Robert H. Cannon

October 1984

Unclassified
SECURITY CLASSIFICATION OF THIS PAGE

REPORT DOCUMENTATION PAGE

1a. REPORT SECURITY CLASSIFICATION Unclassified	1b. RESTRICTIVE MARKINGS None
2a. SECURITY CLASSIFICATION AUTHORITY Unclassified	3. DISTRIBUTION/AVAILABILITY OF REPORT Unlimited
2b. DECLASSIFICATION/DOWNGRADING SCHEDULE	
4. PERFORMING ORGANIZATION REPORT NUMBER(S) SPO Reference 13389-01-00	5. MONITORING ORGANIZATION REPORT NUMBER(S)
6a. NAME OF PERFORMING ORGANIZATION Stanford University 6b. OFFICE SYMBOL (If applicable)	7a. NAME OF MONITORING ORGANIZATION
6c. ADDRESS (City, State and ZIP Code) Dept. of Aeronautics & Astronautics Durand 250 Stanford, California 94305	7b. ADDRESS (City, State and ZIP Code)
8a. NAME OF FUNDING/SPONSORING ORGANIZATION DARPA 8b. OFFICE SYMBOL (If applicable)	9. PROCUREMENT INSTRUMENT IDENTIFICATION NUMBER Contract # F33615-82-K-5108
8c. ADDRESS (City, State and ZIP Code) Air Force Wright Aeronautical Lab Materials Laboratory Wright-Patterson AFB OH 45433	10. SOURCE OF FUNDING NOS. PROGRAM ELEMENT NO. / PROJECT NO. / TASK NO. / WORK UNIT NO.
11. TITLE (Include Security Classification) Second Annual Report on End Point Control of Flexible Robots	
12. PERSONAL AUTHOR(S) Professor Robert H. Cannon, Jr., Professor Thomas O. Binford	
13a. TYPE OF REPORT Annual	13b. TIME COVERED FROM 1 Sept 83 TO 30 Aug 84
14. DATE OF REPORT (Yr., Mo., Day) October, 1984	15. PAGE COUNT 42
16. SUPPLEMENTARY NOTATION	

17 COSATI CODES		
FIELD	GROUP	SUB. GR.

18. SUBJECT TERMS (Continue on reverse if necessary and identify by block number)

Intelligence, manipulators, sensing, control, end-point sensor: flexible manipulators, force control, control algorithms

19. ABSTRACT (Continue on reverse if necessary and identify by block number)

See next page.

20. DISTRIBUTION/AVAILABILITY OF ABSTRACT UNCLASSIFIED/UNLIMITED ☒ SAME AS RPT. ☐ DTIC USERS ☐	21. ABSTRACT SECURITY CLASSIFICATION Unclassified
22a. NAME OF RESPONSIBLE INDIVIDUAL Lt. Mickey Hitchcock	22b. TELEPHONE NUMBER (Include Area Code) (513) 255-7371 22c. OFFICE SYMBOL

DD FORM 1473, 83 APR EDITION OF 1 JAN 73 IS OBSOLETE.

Second Annual Report
on
End Point Control of Flexible Robots
on Contract No. F33615-82-K-5108
Stanford University
October 1984

ABSTRACT

This document reports on progress during the second year of the DARPA contract, whose objectives are "first, to significantly increase the speed and precision of performing 'slew and touch' tasks for a flexible robot arm, and second, to develop a universal robot end effector, capable of performing generic manipulation functions."

Our research concerns key technologies for new classes of robots capable of assembly with force control and great dexterity.

We have achieved end-point control of a very flexible arm, and have demonstrated fast-slew-and-touch motions and the ability to maintain controlled forces at the arm tip using tip-force sensing to control shoulder torques. To do so, we have built a new flexible arm that can be controlled using both optical tip-position sensing *and* tip-force sensing, and have investigated and implemented a switching method between position and force control when contact is made. In this second year we have made some of the improvements to this technology that will be necessary for transferring it to designers of operational robots. Next, we have begun to extend this force-control and force-and-slew capability to a very flexible arm with a "quick-wrist" link at its end. In the coming year we will be in a position to extend the above capabilities for the first time to a two-link arm.

We have built a three finger hand capable of great dexterity. We designed a hierarchical force control system for the hand, with three levels, hand level coupling three fingers, finger level coupling four tendons, and tendon tension level. Finger level and tendon tension control were implemented and demonstrated. During the second year, an analysis was made of rolling objects between fingers. A program was implemented and we demonstrated rolling an egg between two fingers using a relatively general method for object reorienting. We demonstrated coordinated motion of three fingers under the hierarchical control system. A videotape was made which includes segments on both control of three fingers and rolling objects. Work has been underway to improve force control for single fingers to overcome the substantial friction observed.

A flat, flexible 8x8 array of capacitive touch sensors and a second touch sensor array on a cylinder have been fabricated and tested. Preliminary data indicate a clear separation between sensor responses for a cylinder and a wedge.

Table of Contents

INTRODUCTION

This report describes progress in research on intelligent sensory control of end effectors and manipulators. This is a joint research program between the Robotics Laboratory of the Stanford Artificial Intelligence Laboratory (SAIL) and the Aerospace Automation Laboratory (AAL) of Stanford's Aeronautics and Astronautics Department. The joint program operates within the Center for Automation and Manufacturing Science (CAMS).

SAIL reports progress on fabrication of a three finger hand with sensors, on sensory control of the hand, on intelligent task execution with the hand, and on sensor technology. AAL describes progress in force control and fast-slew-and-touch with very flexible manipulators.

These elements of task execution can be termed intelligence, skill, dexterity, and control, going from high-level planning strategy to servo level control. The research addresses three major advances in robots, first force control, second dexterity, and third moving loads at higher speed and precision.

The next major development in industrial robots is likely to be force control, especially in assembly. Robots in industry and in most research laboratories have position control of gross motion, not force control for fine motions in parts mating. The two programs in this joint effort study different aspects of force control of robots, in making contact with objects, in exerting controlled forces on objects, and in making rapid motions of parts for assembly.

Industrial robots and most robots in research laboratories have hands like pliers, i.e. two jaws without sensors with only a single degree of freedom. They cannot grip many objects in many positions, or make stable grasps, or adapt to incomplete information about position and orientation in grasping. Three fingers with the necessary freedoms and with force sensing support are now capable of grasping curved objects in many positions, grasping them stably, adaptive grasping, re-orienting objects, and fine motion for parts mating and force control.

We study intelligence in grasping strategies and in parts identification by grasping.

We also study control methods that can contribute to lowering the cost of using robots by making them fast and increasing their payload despite limited strength and despite flexibility. Current robots are made stiff enough and strong enough to ignore loads. A Unimation PUMA weighs 120 pounds and carries a payload of five pounds. Unavoidable flexibility in drive trains of robots and in their mounts make precise end-point control of flexible robots an issue of central importance.

In the second year, we have concentrated our efforts on object manipulation, tactile sensing, and improved finger force control. We demonstrated rolling an egg between two fingers. We demonstrated simultaneous motion of three fingers. A videotape includes both demonstrations. Progress has been made toward higher bandwidth servos and to improve force control of fingers.

An 8x8 array of capacitive touch sensors has been fabricated and tested. They appear promising for use on the hand. A 12 channel electronic interface was built for motor control and is coming into use. The SAIL laboratory was moved and put back in working order.

We have modified the single, very flexible beam and its controller in some ways that make the technology more directly transferable, and we have begun to document the theory underlying this achievement.

We have designed and nearly finished construction of a new, very flexible beam with a quick wrist at the end, with which we plan soon to demonstrate much more versatile slew-and-touch technology, and we have begun the control theory and simulation aspects of this project.

We have begun to extend the theory of end-point force control and of slew-and-touch tactics to the two-dimensional case in preparation for the demonstration with the two-link arm that we plan for the third year.

AN OVERVIEW

In our First Annual Report (Ref. 2) on this DARPA contract we provided an overview of all of our work on intelligent, dextrous hands, and very flexible manipulators, of which the DARPA portion focusing on force control and slew-and-touch maneuvers is a key part. We provide here a much shorter version of the overview, for context.

Intelligence and Force Control of Dextrous Hands

This research is aimed at understanding and developing motion capabilities in generic assembly which include: 1) tool using; 2) parts acquisition; 3) parts handling; 4) parts mating. Force control and compliance are crucial in generic assembly operations. These generic assembly operations depend upon generic motion capabilities which include: 1) grasping securely; 2) repositioning objects; 3) controlling and exerting delicate forces; 4) making fine motions.

Secure grasping is important for tool using and for rapid motion. A hand with parallel jaws can grasp an object in only a few configurations, e.g., at parallel faces. The three finger hand with nine degrees of freedom can grasp a broad class of objects in a range of configurations. Also, a hand with two parallel jaws can supply very little torque about the axis between the jaws. Thus, an object swings easily about this axis when moved rapidly or under small external forces.

In parts acquisition, e.g., bin picking, it is often necessary to grasp objects then reposition them for assembly. Two finger hands with one degree of freedom are kinematically incapable of repositioning objects. The three finger hand was designed with the degrees of freedom necessary to reposition objects fully in space, i.e., to rotate and translate them.

In force control, not only is force sensing important, but the device itself must be capable of fine force control. Fine motion devices provide the fine control which is not possible to achieve by working with the large joints of the arm. Humans typically perform fine operations by resting their wrist on a flat surface and acting with the fine motions of the hand, rather than working from the shoulder and compensating for the weight of the arm. The hand is instrumented to sense tendon tensions and to compensate for friction. Friction is a major obstacle in controllability. The hand was designed for fine motion. It was also designed to minimize friction by a pull-pull tendon design.

The hand provides fine motion to respond rapidly with small motions to accomodate errors measured with visual sensors and force sensors in close tolerance work.

Rapid, Precise Position and Force Control of Flexible Manipulators

Manipulators — arms and hands with their actuators, and the increasingly sophisticated feedback systems that control their movements — are the "business end" of a robot, where parts are mechanically moved, formed, placed, fitted together (or dismantled), and inspected. In our Controls Group we are addressing the question of how to provide manipulator control so good that a whole new generation of manipulators can be developed — manipulators that are much lighter and far more facile than anything today's control systems could stably manage.

The central control problem for each of these manipulator systems — and the problem we have been the first to solve — is the problem of controlling the end-point (fingertips) of a manipulator by measuring position or force *at that point* and using *that* measurement to control torque at an actuator at the other end (elbow or shoulder) of the flexible manipulator. This turns out to be, for fundamental stability reasons, *very hard to do*. Every time someone has tried it (this *noncolocated* control) in commercial robots, the robot system has gone unstable.

Using advanced control methods developed in our laboratory we have already succeeded in achieving for a very flexible beam, control that is not only stable but highly robust, and at a speed limited basically by wave propagation times in the manipulators themselves. The first achievement of near-wave-propagation-speed control was accomplished for optical control by Eric Schmitz, under NASA funding, and for force control by James Maples, under this DARPA funding. Maples achieved both force control *per se* and initial demonstrations of fast-slew-and-touch control.

During this second year two additional major capabilities have been attained first at a fundamental level under AFOSR support, and we will now be able to use each of these to develop and demonstrate force-control and slew-and-touch capability in a much broader context. One of these is a quick-acting wrist for the end of our very flexible beam, with which very fast local motions can be accomplished, thus completely circumventing the wave-propagation-time problem of the carrying beam. The other is a two-link arm with flexible tendons, with which we will begin force-control and slew-and-touch control in two dimensions.

Also under AFOSR funding we are now beginning some very fundamental experimental work in adaptive control of flexible systems; and this will provide a new dimension of theory upon which future DARPA work can draw.

A most important fact is that the gratifyingly rapid progress we have been able to achieve in each of the projects is due in great measure to synergism with the *other concurrent* projects in whose midst it exists. *The combination of major funding indicated in Fig. 2 of Ref. 1 has made possible a critical mass of talented people and new equipment and activity, without which many of the achievements of this year would simply not have occurred at all, let alone so quickly. The presence concurrently of all these people is what has made these achievements happen.*

Again, the basic generic thing that we have been able to do (and be the first to do) is control very light, flexible manipulators in swift, purposeful motions: control position and force at their tips by measuring these quantities directly and feeding them back.

Report on Research

I. INTELLIGENCE AND DEXTERITY IN FORCE CONTROL OF A THREE FINGER HAND

This document reports on progress during the second year of the DARPA contract toward objectives of developing dexterity in generic manipulation tasks, using the Stanford/JPL three finger hand. Our research concerns key technologies for new classes of robots capable of assembly with force control. The three finger hand provides unusual capability for generic motion capabilities to support assembly: 1) secure grasping; 2) repositioning and reorienting objects; 3) exerting small, controlled forces; and 4) making rapid fine motions.

In the first year, we completed construction of a three finger hand with nine degrees of freedom, capable of completely repositioning and reorienting an object for small motions, and capable of exerting small, controlled forces. We designed a force control system for it which is novel in that it controls object motion, i.e. position, orientation, and forces exerted on an object. Commanding object motion instead of joint motion is natural for high level, task-oriented planning systems. The control system has a three level hierarchy, namely hand level, finger level, and joint level. Two levels of the control system were implemented, i.e. finger level and joint level control. Control of one finger of the hand was demonstrated.

Also during the first year, we made progress toward an intelligent system for grasping objects and manipulating them. One effort investigated rolling and slip in manipulation without models of the object. Work was begun on another system which uses object models in identifying objects and orienting them in grasping.

In the second year, we have concentrated our efforts on object manipulation, tactile sensing, and improved finger force control. We demonstrated rolling an egg between two fingers. The method for object reorienting is reasonably general; work has begun to extend it to straight generalized cylinders with constant cross section. We demonstrated simultaneous motion of three fingers. A videotape was made which includes segments on both control of three fingers and rolling objects. Work has been underway to improve force control for single fingers to overcome the substantial friction observed.

A flat, flexible 8x8 array of capacitive touch sensors and a second touch sensor array on a cylinder have been fabricated and tested. Flexible, compliant finger covering is important for grasping. An analysis has been carried out for inferring surface forces and deflections from sensor signals. Sensors are 1.5 mm on a side. They are read at 10 Hz now. They are at least sensitive enough to detect 1 gm/sq cm. Preliminary data indicate a clear separation between sensor responses for a cylinder and a wedge.

A 12 channel electronic interface was built for motor control; the hand will be interfaced using it for future experimentation. The interface has proven to be preferable to the Unimation interface.

Also during the second year, the laboratory was moved and put back in working order. This meant a complete changeover in our computing environment from direct connection to a time-sharing DEC 20 system and a VAX-UNIX system to remote operation over a

branch Ethernet and gateway. Considerable effort was required to debug the PDP11/60 and PDP11/45 after the move.

Work was continued on object recognition using object models. A section in this report describes a modeling system which is partially implemented based on halfspaces bounded by quadric surfaces (2nd order).

Much work still needs to be done on the analysis of tactile data, planning object manipulations using tactile data, and developing general manipulation capabilities.

In the coming year, we plan the following: 1) mount the hand on a Puma 560 and carry out coordinated coarse and fine motion, i.e. fine motion control of the hand about a coarse motion of the arm, providing extended fine control; 2) perform delicate force control of extended motions using combined coarse control of the arm and fine control of the hand; 3) mount an 8x8 tactile sensor array on each finger and conduct grasping experiments; 4) improve tension control of fingers by speeding up calculations; 5) extend parts reorienting to straight generalized cylinders with constant cross section; demonstrate parts reorienting using three fingers; 6) refine and implement hand level control which coordinates the motion of three fingers to implement object motions.

During the past year, we have concentrated our efforts on Object Manipulation, Tactile Sensing, and improved Finger Force Control. Figure I-1 shows the specific tasks that we see as necessary to achieve intelligent dexterity. Past research has led to the next projects: improved force control and higher bandwidth servos; three finger hierarchical, coupled control and its use in three finger object manipulation; mounting the hand on a PUMA and developing combined coarse and fine motion; developing a tactile sensor array and adding sensor arrays to the fingers; using sensor arrays to estimate local properties of surfaces.

Much work still needs to be done on the analysis of tactile data, planning object manipulations using tactile data, and developing general manipulation capabilities.

Manipulating Objects

Fearing analyzed rolling polyhedra between two fingers. This rolling operation gives the ability to re-orient an object in the hand while maintaining a quasi-stable grasp. The goal of this work was to show the feasibility of using fingers with stiffness control and limited slip to manipulate small parts within a hand.

The photos in Figure I-2 show a rectangle grasped with a fixed upper finger, and force controlled lower finger. The lower finger is commanded to apply a force radially directed into the contact point at the upper finger. A high stiffness in the tangential direction keeps the finger aimed toward the upper finger contact point. The object is stably grasped because the forces are within the friction cone and the object is in equilibrium, i.e., the reaction force at the upper finger is equal in magnitude, colinear and oppositely directed to the applied force.

To cause object motion, a tangential time-varying bias force is added to the controlled finger. This tangential force generates a moment about the fixed finger, causing the object to rotate about the contact point. There may be slip at either finger, but the radial

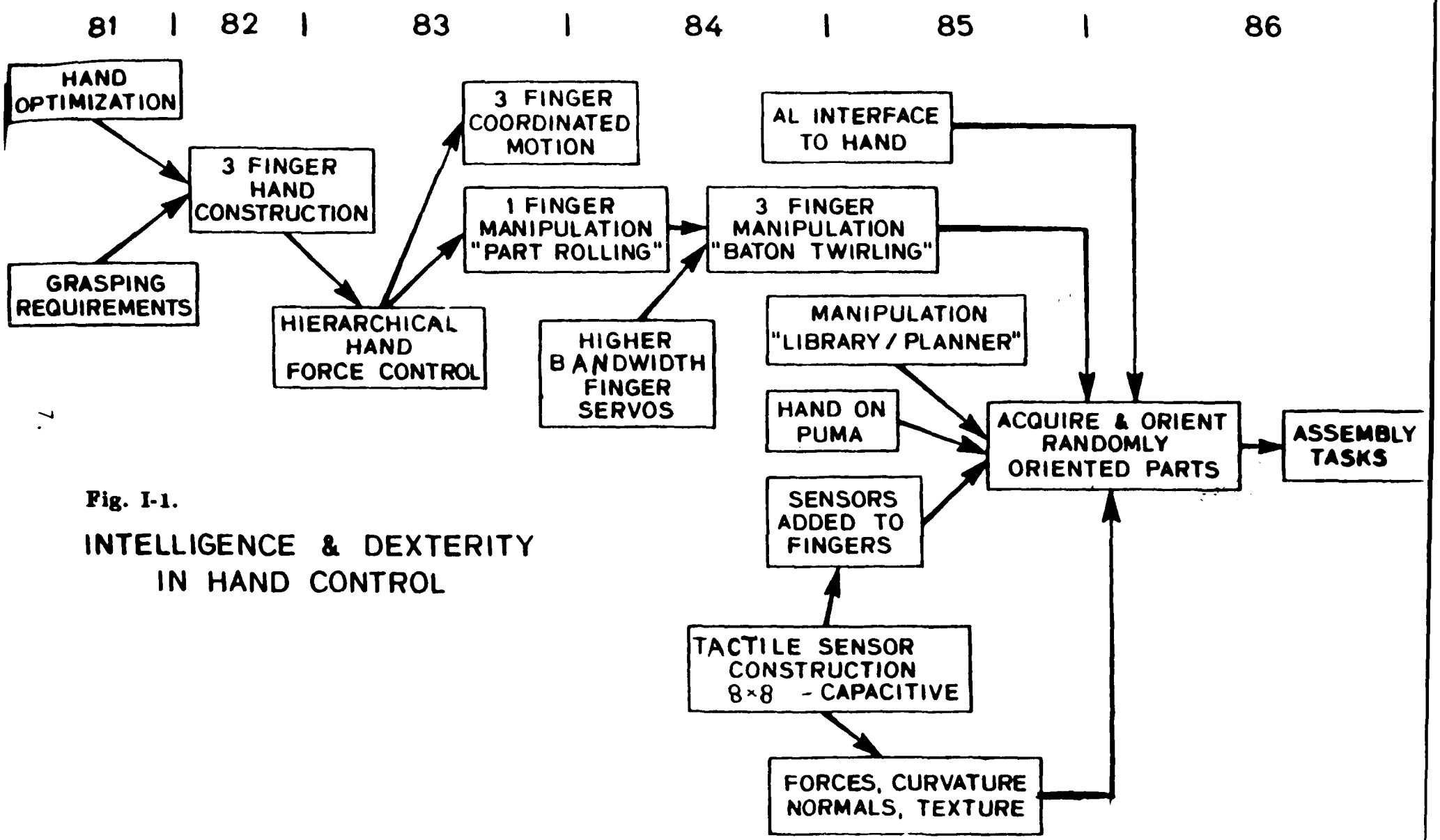

Fig. I-1.

INTELLIGENCE & DEXTERITY
IN HAND CONTROL

A

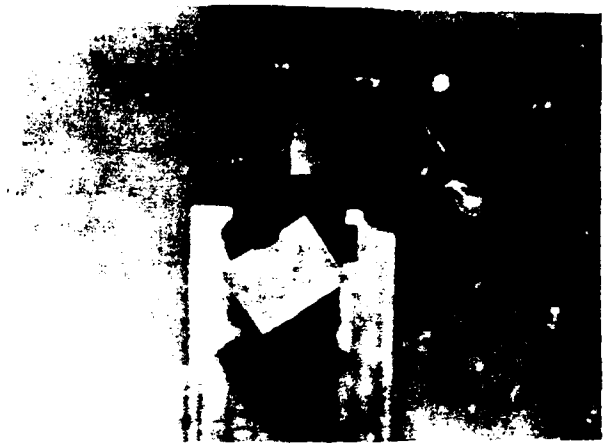

B

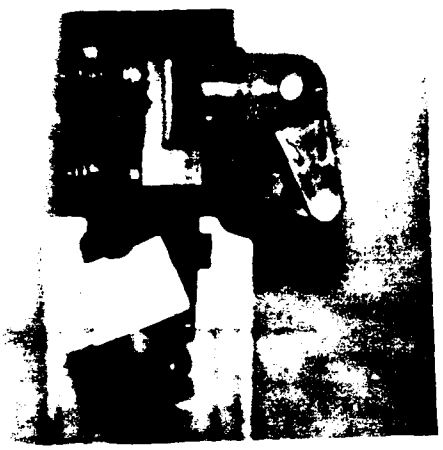

C

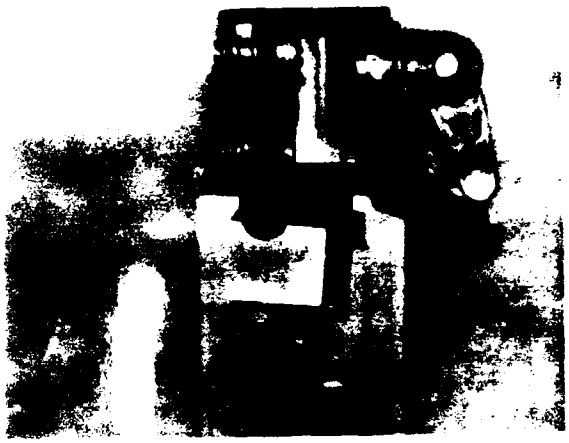

D

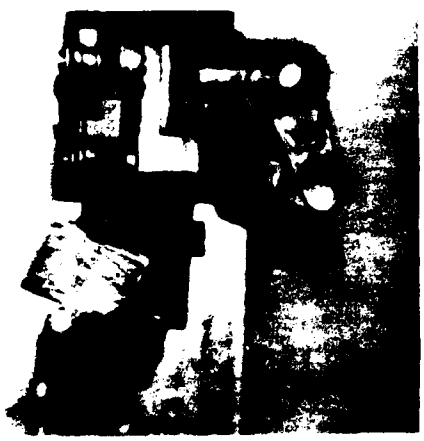

E

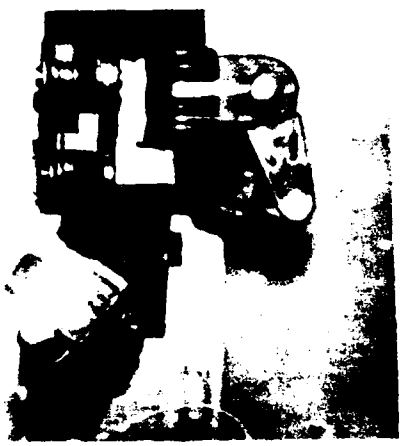

F

Figure 1-2 Manipulating a Rectangle

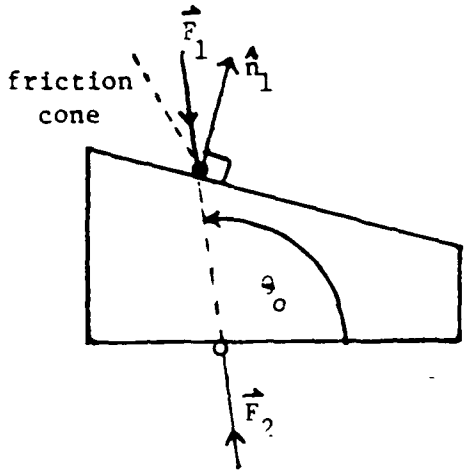

A. Stable Grasp

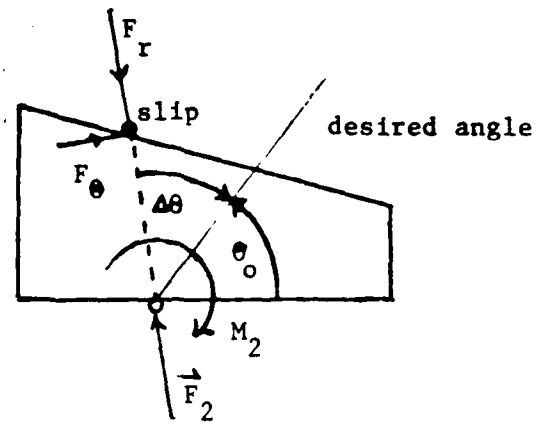

B. Extra Force at Finger 1

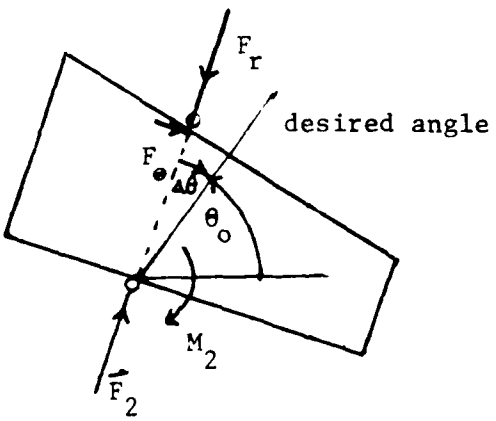

C. Slip at 1 and Rotation at 2

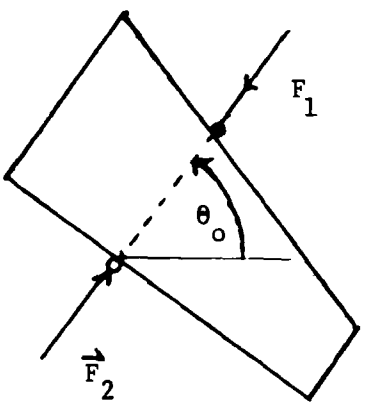

D. New Stable Grasp

Fig. I-3. Part Rolling.

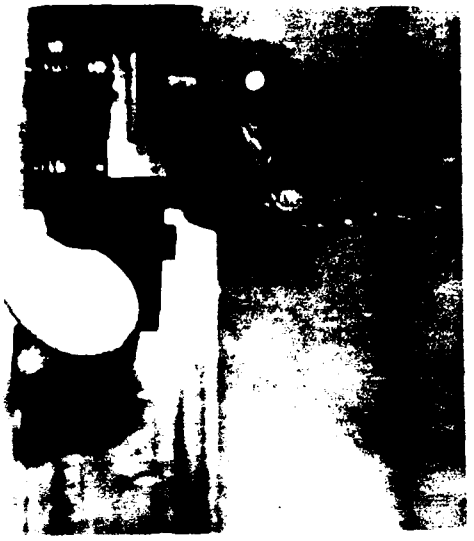

A

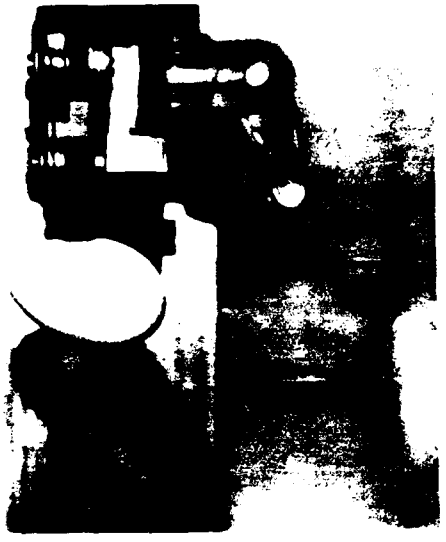

B

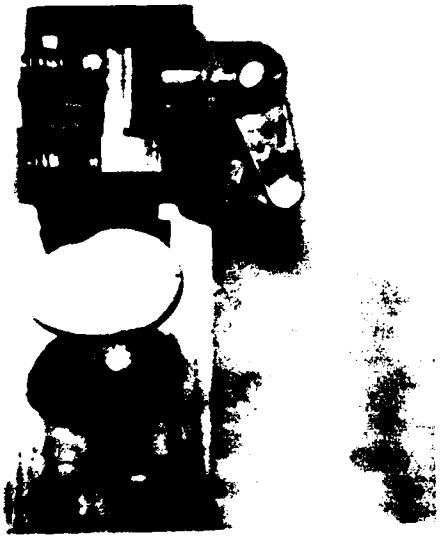

C

Figure 1-4 Manipulating an Egg

force control scheme keeps the object from escaping from the hand. Figure I-3 depicts the applied forces and resulting object behavior. The general approach to using slip and finger stiffness control was described in [Fearing, 1984].

We have started to extend this method from polyhedra to straight generalized cylinders with constant cross section. With two fingers and slight friction, finger placement becomes critical for a stable grasp. We have shown that there are always two pairs of finger locations where a stable grasp is possible. Using finger stiffness control, one of the pairs will result in a more stable grasp. If the radius of curvature of the object contour is greater than the inter-finger distance, then finger slip will cause the fingers to move further apart. As the fingers separate, work is done to increase the virtual potential energy of the equivalent springs of the stiffness control system. Since object slip requires work against the control system, and the stable configuration has the lowest virtual potential energy, slip will tend to be inhibited. We have taken advantage of this fact to demonstrate manipulation of an ellipsoidal object in Figure I-4.

It is important to note that these examples do not require any object model, just the magnitude of the force to be applied to compensate for gravity.

We have found that some manipulations, like translating a pencil with just two fingers, may require control of friction at the two contact surfaces. This can be done by changing the contact area. (The greater the contact area, the larger the effective friction coefficient.)

Sensing

In the near future, we anticipate using tactile data to direct grasping operations, by distinguishing low level features like object edges, vertices, and sides, and determining forces and object locations in the hand. In order to begin working with real tactile data, we have constructed a prototype 8x8 flexible tactile sensor array. Flexibility is very important, because for object manipulation, we will need to have curved fingers with compliant coverings.

The sensing mechanism is the deflection of capacitor plates. Each capacitor is formed at the intersection of 1.57 mm wide crossed strips, which are separated by a compliant dielectric. Each element of the 8x8 array is about 1.5 mm on a side. Using multiplexers, one row is excited by a 10 volt 100 kHz sinusoidal drive signal. The output is read from one column, amplified and detected to give a DC output signal inversely proportional to the capacitor deflection. This sensing scheme was inspired by a capacitive tactile sensor described by Boie [1984]. Because the capacitance at each crossover is only about .1 pF, connections from the sensor to the first amplifier stage must be very short.

The entire array is scanned at a 10 Hz rate. This can be increased when we start "structure from motion" experiments, where a finger is dragged along an object without stopping. Dynamic tactile sensing will require a fairly high CPU bandwidth.

Figures I-5a and 5b show the prototype planar and cylindrical versions of the sensor. Work is currently underway on choosing appropriate dielectric, conductive and compliant materials that will give a more homogeneous and sensitive sensor. We hope to have a sensor that can be modelled well enough to make accurate predictions of surface forces and deflections from the sub-surface deformation.

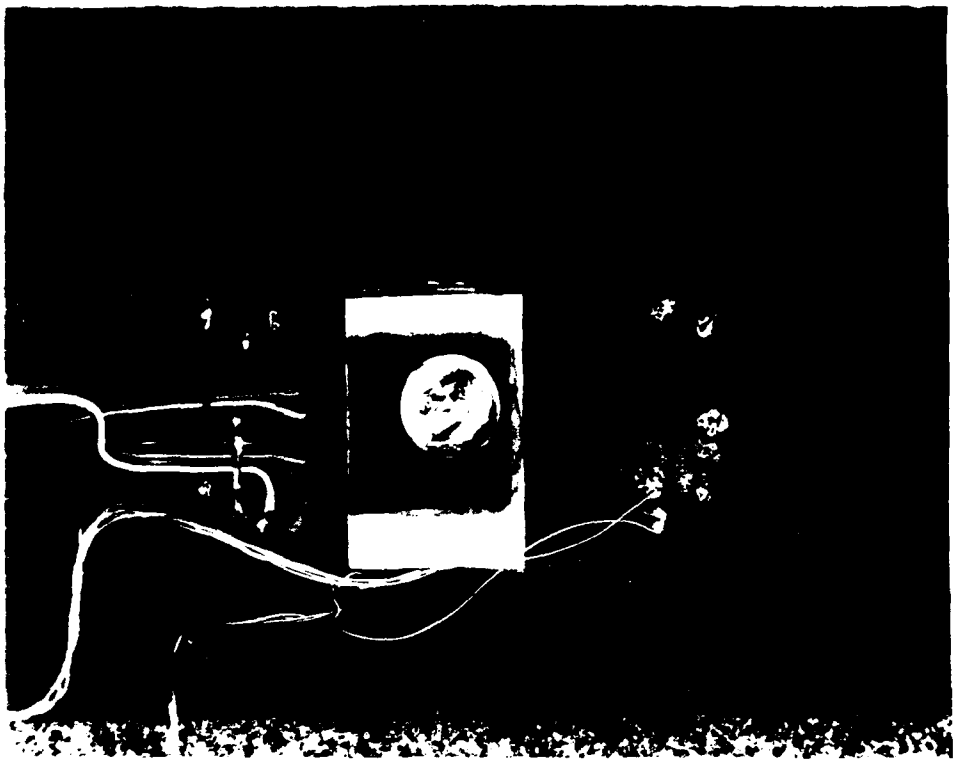

a) Planar 8x8 Array

b) Cylindrical 8x8 Array

Figure 1-5 Prototype Tactile Sensors

Fig. I-6(a). Single cell response for load on 0.25 inch diameter probe (7.9mm^2).

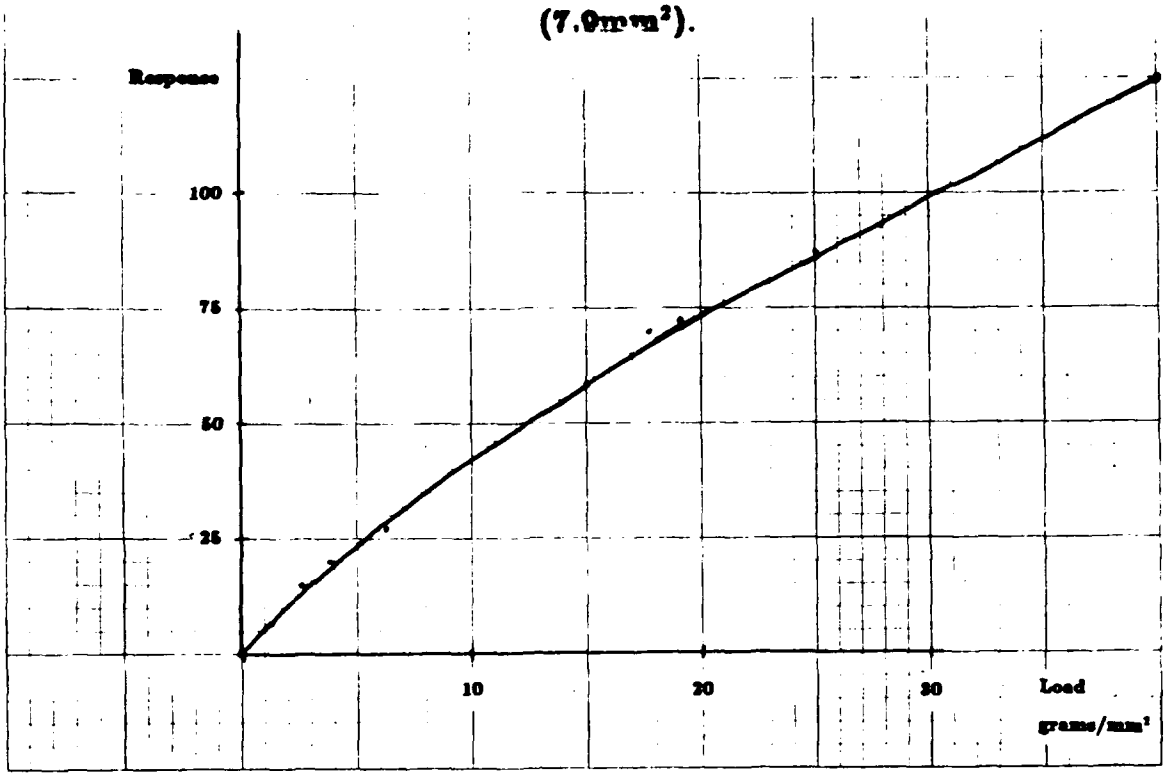

Fig. I-6(b). Single cell response for load on 1 cm. x 1 cm. square.

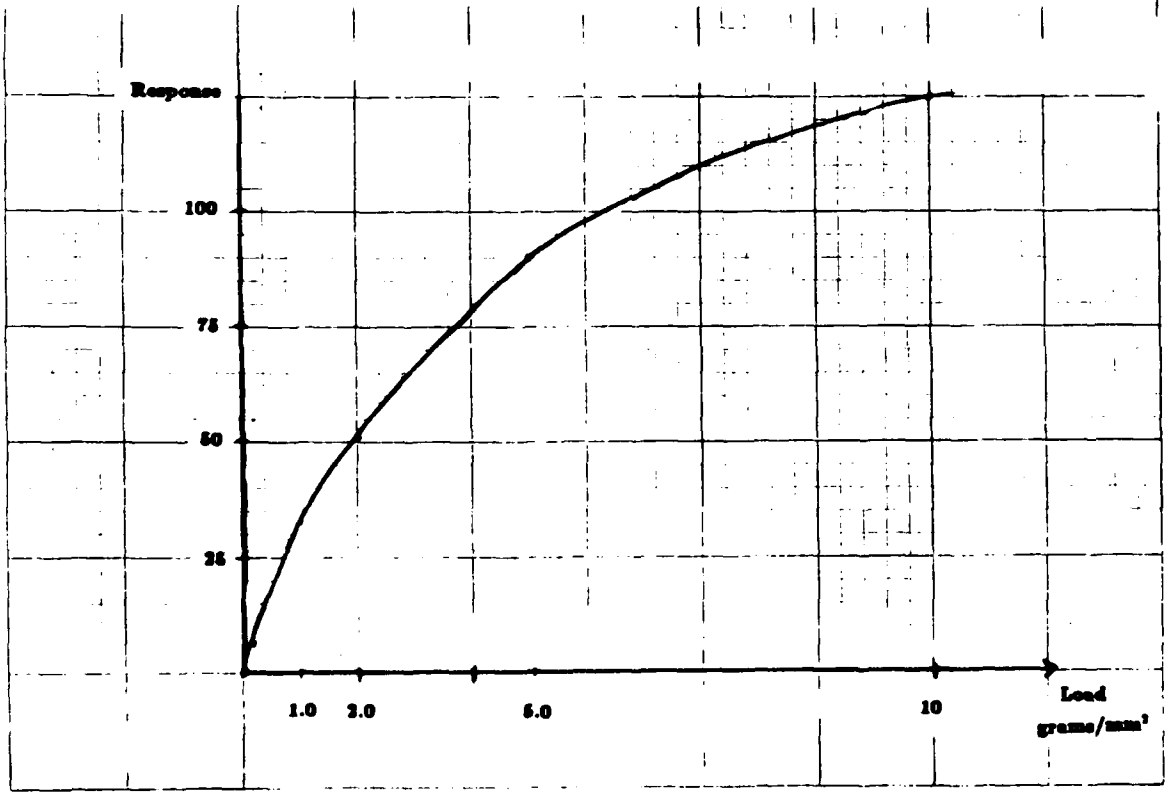

Figure I-6a shows a typical response to a point load with increasing pressure for the planar sensor. The response is monotonic and fairly linear for small loads, with decreasing sensitivity for larger loads. The small probe diameter (area of 7.9 sq. mm.) lowers the effective sensitivity, because it is likely to be between two capacitors, rather than centered over one. Figure 6b gives the response for a larger contact area of 100 sq. mm. This response is less linear, but also more sensitive. A likely explanation for this is that a larger volume of compliant material is being displaced, so we are no longer in the domain of linear elastic properties.

Figure I-7a shows the sensitivity with a large contact area, in this case a penny with just its own weight that is two thirds on the active sensor area. In this figure, the sensor data is multiplied by 16 to show off the low level signals. The low force threshold on this prototype is about .1 g/ sq. mm. when the contact covers several cells. All photos of the sensor gray level output were made by simply substracting each cell's zero pressure output offset from its response. No adjustments for individual cell gain variations were made.

Preliminary experiments have shown a noise level of about 1 percent of the full scale signal, or about 7 bits of force resolution. The noise determines the limit on the effective spatial resolution of the device, and can be reduced with improved shielding on the sensor and interface electronics.

Figures I-7b and 7c show a cylinder and a wedge (edge contact) contact on the planar sensor respectively. As Figure I-8 and 9 indicate, these two contacts can be discriminated by the width of the response profile they generate.

The cylindrical geometry of a curved finger will make the deformation more difficult to analyze. By using a thick skin, we should be able to use locally planar approximations and linear elasticity theory to predict the sensor response. Figure I-10 shows the response for the cylindrical finger contacting a flat surface. A thicker skin would give more information here.

We plan to put one 8x8 sensor array on each of the three fingers of the Stanford/JPL hand. There will be a local amplifier and multiplexer at the base of the finger, with just a few high level control and signal connections going off the hand to the computer.

Control

Early in the second year, Craig demonstrated simultaneous manipulation of three fingers. This capability was demonstrated in the videotape.

A 12 channel electronic interface was constructed for interfacing motors to a Unibus. It has a bus interface card which selects individual channels. Each channel reads incremental optical encoder input and provides a D/A conversion with constant current output to motors.

Our part rolling experiments pointed out several deficiencies in our current finger control scheme. The main problems were excessive control loop calculation times, and poor quality force control.

We have demonstrated controlling three finger positions simultaneously. However, our computational power has not been adequate to control three finger forces simulta-

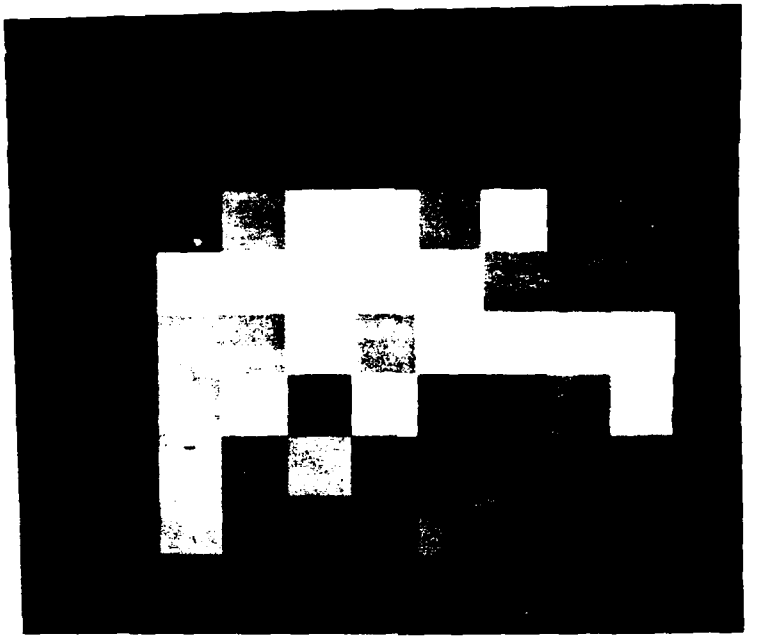

a) Penny under own Weight (gain x 16)

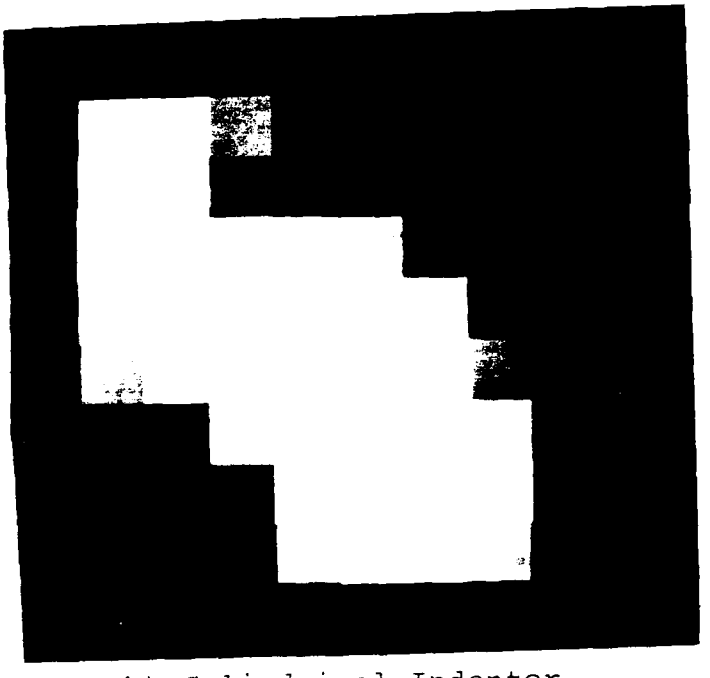

b) Cylindrical Indentor

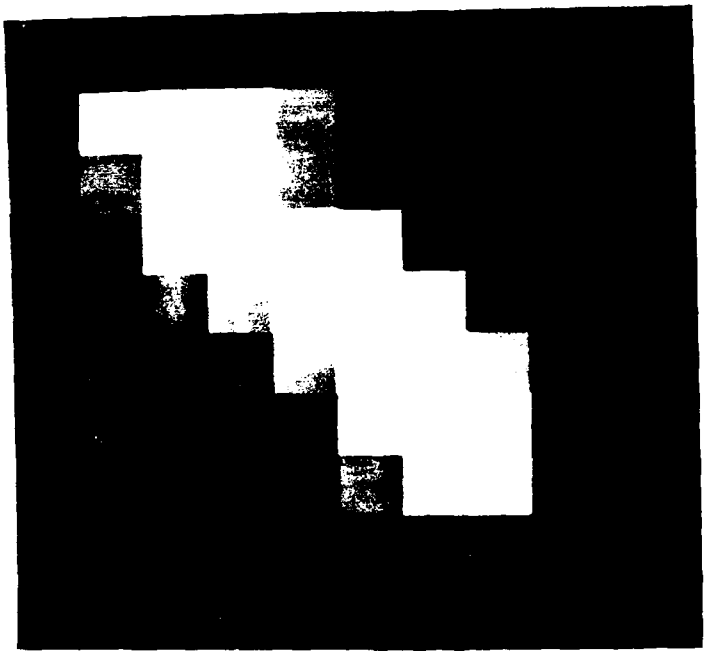

c) Wedge Indentor

Figure 1-7 Planar Sensor Responses

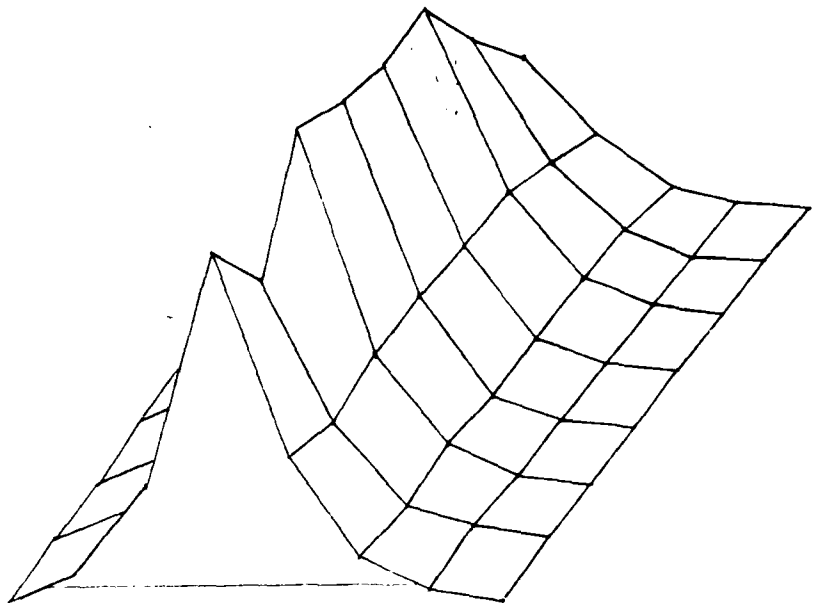

Fig. I-8. Response for Wedge Indentor.

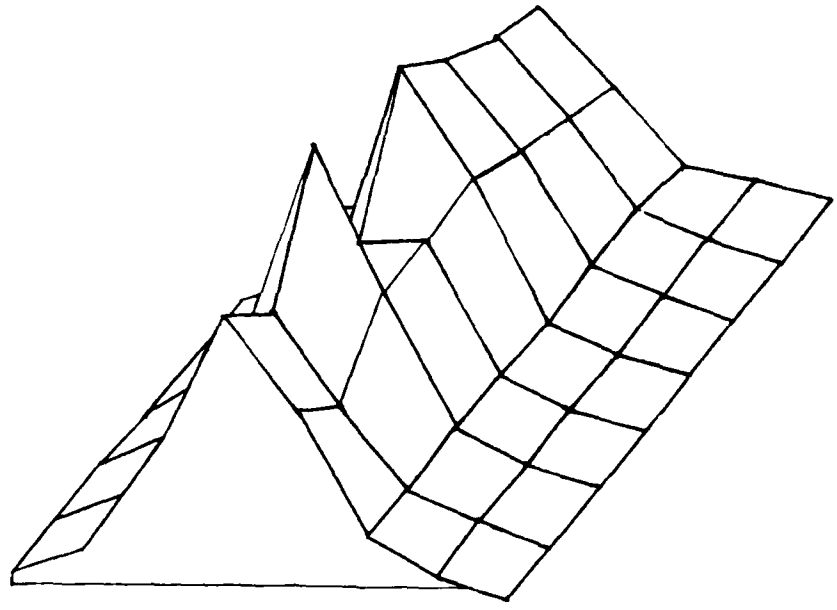

Fig. I-9. Response for Cylindrical Indentor.

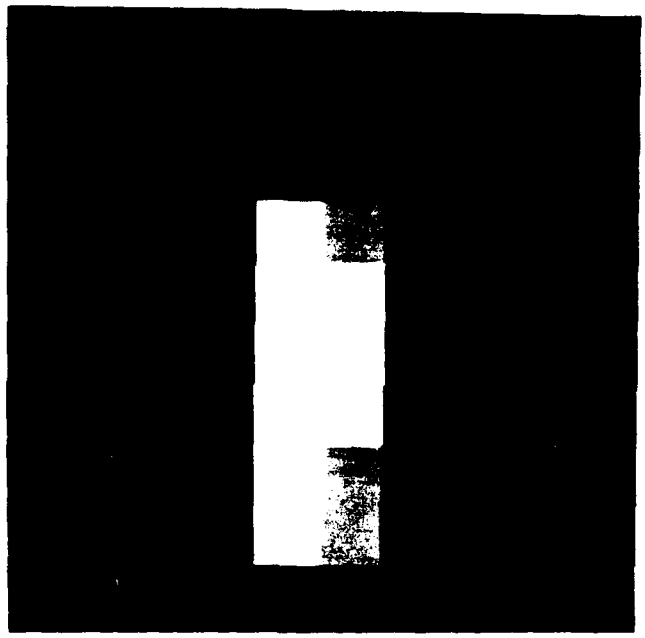

Figure 1-10 Cylindrical Sensor with Planar Contact

neously. To speed up the control calculations, the three finger hand was moved to the PDP-11/60 which is twice as fast at floating point calculations as the PDP 11/45. We are also experimenting with a joint-based stiffness scheme to control finger forces that does not require constant recalculation of the Jacobian matrices, which have a lot of overhead with trigonometric calculations. In this scheme, a three by three stiffness matrix, with terms and cross-coupling for each joint stiffness is derived that approximates the desired force characteristic at the finger tip as a function of finger position. These improvements should allow adequate CPU bandwidth for simultaneous force control of all three fingers.

Burdick has implemented a data passing procedure between the two PDP-11s using direct memory access hardware. This looks very promising for putting the high level, low rate processes, such as determining finger stiffness matrices, on the 11/45, and leaving the 11/60 free to run the low level servo at maximum speed.

To control the finger force vector in cartesian space, we map cartesian finger tip forces to joint torques using the Jacobian matrix. We have been controlling joint torques by commanding tendon tensions. With commanded tendon tensions of around 1000 grams, responses were very sluggish. Combined motor, brush, gear and tendon friction is about 1500 grams, which results in a minimum controllable force at the end of the finger of about 100 grams. For comparison, a PUMA arm with a force wrist controlled by the COSMOS system can apply a minimum force of the order of 200 grams, so there is much room for improvement for the finger force control.

The sensed tendon tension for low static tendon tensions is mostly due to friction, and not applied motor torques. To overcome the friction problem, we are implementing a new force control scheme that calculates current joint torques from the tendon tension sensors, and commands a joint velocity that is proportional to the joint torque error. This puts the control problem in position space instead of force space, so the friction problem is less severe.

Since the joint velocity maps directly into motor velocity through a constant transformation, the low level underlying servo is now a motor velocity servo instead of a tendon tension. The Unimate controllers are designed to control a motor torque, or a motor position; they are not designed to implement a velocity servo loop. In torque mode, they have an overhead of about 200 us per motor to read its encoder, or to send a torque. This significantly reduces the overall servo rate when twelve motors have to be run.

For expediency, the new 12 channel motor interface was substituted for the Unimate controllers. We will now implement a motor velocity control using the 11/60 to servo motor torques. This should run quicker than with the Unimate controller, and we now have direct control over motor velocity instead of having to feed the Unimates an incremental position command to simulate motor velocity control.

Preliminary results in the "float" mode seem promising: when zero joint torque is commanded, the finger is much freer than under the previous servo scheme.

Constructive Solid Geometry Using Quadric Halfspaces

Constructive solid geometry on quadric halfspaces is an approach to modeling which offers generality in a concise framework. The implementation, however, is neither straight-

forward nor efficient.

Primitive models are halfspaces representable by quadric equations. Solution of a quadric for a given point in space yields a value ¿0, =0, or ¡0, when the point is inside, on, or outside of the quadric surface, respectively. "inside" and "outside" are set inclusion and exclusion, and provide a basis for the creation of more complex models by arbitrarily applying complement, union, intersection, and difference operations to primitive halfspaces and models built from them. Set operations on these models are complicated by the existence of points on the boundary between a halfspace and its complement. These points cannot be ignored, as they become the boundaries of the model.

A model is a collection of volumes, faces, edges, and vertices. A volume is the intersection of halfspaces, and a point lies in the volume if it satisfies the equations for each of the quadrics defining the halfspaces. A face of this volume is a part of one of the quadric surfaces that define it, has solution =0 for that quadric, and has solutions for all the other quadrics in the volume. An edge is that part of a space curve defined by the intersection of two quadric surfaces (solutions =0) but within the volume with respect to the other quadrics. A vertex is the intersection of three quadrics.

The overriding practical necessity is the identification of null elements: volumes, faces, and edges satisfied by no points in space. As the number of quadrics that contribute to a model grows linearly, the number of potential elements grows exponentially, while the number of non-null elements remains approximately linear. As a model is constructed, null elements must continually be identified as such and eliminated from the representation. The formal representation of an element is unsuitable to this problem, as it would require the determination as to whether or not a simultaneous solution exists for any number of quadric inequalities. Even the only finite case, that of finding possible vertices, is a system of three equations having an eighth-order solution.

An alternative representation is of elements as collections of discrete points. An edge becomes a list of adjoining line segments. This approach has the obvious drawback of being a somewhat inefficient representation, and as well requires specific definition of the infinite and infinitisimal. Vertices may be found as the intersection between an edge and a quadric surface, by interpolating between any sequential pair that are found to lie on opposite sides of the surface. Generating space curves numerically is a fourth-order problem in the worst case. Once a curve is generated, it may be pared down to an edge by testing each point with each of the quadrics defining the specific volume. If none of the points pass, then the edge is null. The numerical approach does not extend easily to two or three dimensions, for representing faces and volumes, however.

Some use may be made of the geometric relationships between an element of a model and its bounds. For example, a non-null volume is bounded by non-null faces. A face has no bounds if it bounds a primitive half- space, otherwise its bounding edges must be non-null if it is non-null. Similarly, an edge has no bounding vertices if it is a complete space curve (not constrained except for the two quadrics that define it), and must have bounding vertices otherwise. By using the discrete representation of edges and vertices, null edges are known, and null faces and then volumes may be discovered, except in some special cases.

A complex model is built up by performing a set operation on two simpler models,

starting with primitive halfspaces. For the binary operations, each of the operand models is divided into two: a sub-model that is a subset of the other model, and a sub-model that is disjoint. Two or more of these four sub-models are combined together to form the product. If models are structured as trees according to an arbitrary hierarchy of the quadric surfaces that define it, operations may be performed more efficiently, although several nested recursions are necessary in any case. The essential elements are volumes, the other elements must be associated with the elements that they bound. In special cases "dangling" faces and edges bounding nothing, may be found, but must not be included in the product model. Another example of a special case is a face bounding two volumes, and therefore interior to the model. For efficiency's sake both volumes and their common face should be combined into one volume, although this may not be desirable under certain applications.

Plans

In the next year, we intend to demonstrate object re-orientation and regrasping using simultaneous force control of three fingers. Only independent motion of three fingers has been implemented thus far. Our first task will be twirling an object; grasping an object with two fingers, using the third finger to apply a disturbance force that rotates the object, and then regrasping the object with the second and third fingers.

By combining manipulation procedures like part rolling and twirling, we will be building up a library of general manipulation commands that will eventually allow arbitrary re-orientation of objects within the hand. This dexterity is necessary for assembly tasks.

We plan to mount the hand on a PUMA arm. Within the next several months, we intend to study how the three finger hand and PUMA arm can work cooperatively when the hand is mounted on the arm. The initial task division will be for the arm to make coarse motion in the vicinity of the target path, and for the hand to make the fine motion for final contact and fine motion along the path for finger force control. A very important problem is protecting the fragile hand from collisions with unforeseen obstacles. Proximity sensing on the arm to stop quickly when near an obstacle will probably be needed.

We plan to mount a tactile sensing array on each finger of the hand and to incorporate tactile sensing in manipulation strategies and control.

References

[1] R.S. Fearing, *"Simplified Grasping and Manipulation with Dexterous Robot Hands"*, American Control Conference, San Diego, CA, June 1984.

[2] R.A. Boie, *"Capacitive Impedance Readout Tactile Image Sensor"*, IEEE International Conference on Robotics, Atlanta, GA, March 1984.

II. FORCE CONTROL OF VERY FLEXIBLE MANIPULATORS

Because this DARPA contract is supported by 6.2 class funds, our emphasis has been a bit more toward *demonstrating* a series of robotics control technologies, and a bit less toward underlying theory. (Indeed, we have drawn heavily upon the strong and now-widely-used body of control theory that has been developed at Stanford, and which is *currently* developing here — especially in our laboratory — under funding of the 6.1 class.) Even so, we intend to document carefully the theoretical basis that is making our series of DARPA demonstrations possible, first because such theoretical understanding is essential to effective transfer of the technology, and second, because in fact this work is itself necessarily producing some key new contributions to control theory *per se*.

In this spirit, we describe here the new capabilities we have been able to demonstrate experimentally in the second year of this contract, providing, as we do so, reference to the underlying theory. Some new contributions to the theory are detailed in Appendix A. By the end of the third year we expect to submit a major, stand-alone report on the theory and experiments in flexible beam slew-and-touch technology.

In particular, this DARPA-supported research is focused on demonstrating new capabilities for touch and force control, on slew-and-touch control, and on the extensions of control theory necessary to achieve them.

In the first year we made progress in two areas:

1. With a single, very flexible beam equipped with both an optical and a force sensor at its end point, we achieved (all for the first time anywhere) noncolocated high-bandwidth force control, (b) fast, smooth slew-and-touch, with switching from optical to force control (without pause), and (c) slew-and-touch to a moving target with the same features as (b).
2. We designed and constructed a two-link robot arm with flexible tendons, using joint DARPA and Air Force funding. Optical end-point control of the arm will be developed under Air Force sponsorship, and *force* control of the arm will be developed under this DARPA funding.

During this second year we have made progress in three areas:

1. We have modified the single, very flexible beam and its controller in some ways that make the technology more directly transferable, and we have begun to document the theory underlying this achievement;
2. We have designed and nearly finished construction of a new, very flexible beam with a quick wrist at the end, with which we plan soon to demonstrate much more versatile slew-and-touch technology, and we have begun the control theory and simulation aspects of this project;
3. We have begun to extend the theory of end-point force control and of slew-and-touch tactics to the two-dimensional case in preparation for the demonstrations with the two-link arm that we plan for the third year.

In the paragraphs that follow, we describe our progress in these areas in the context of the task statements of our DARPA contract.

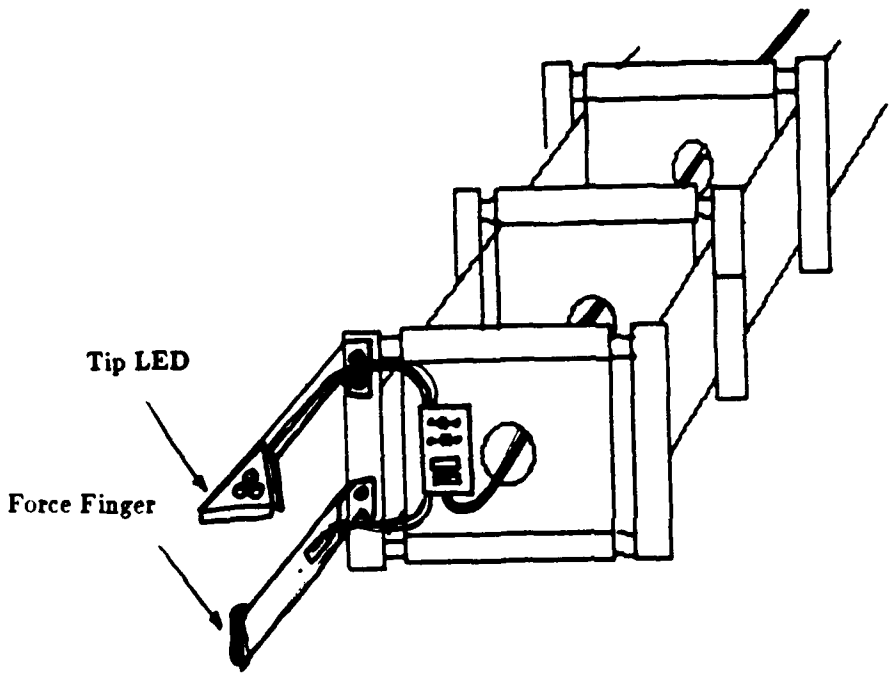

Figure II-1 Modification of Force Sensor Mount

Task 1 (4.1.1) Develop a Minimum-Time Algorithm for "Slew-and-Touch" of a Single, Very Flexible Manipulator.

In year 1, Jim Maples accomplished all of this task, in a first iteration, directing a highly flexible (0.5 Hz), one degree of freedom, robotic arm, through a fast, large angle motion toward a target object (subtask 4.1.1.1) and contacting the target object without pause in the motion of the robotic arm (subtask 4.1.1.2), with relatively high velocity at the instant of contact (subtask 4.1.1.3). The absolute time-delay limit to system response was identified as the wave propagation time in the beam, about 100 milliseconds, (subtask 4.1.1.4), and the required system bandwidth was established at about 1.2 Hz (subtask 4.1.1.5).

The equipment used in the first year demonstration is shown in Figure 4 of Ref. 2. As the figures shows, as a convenient expedient for those first experiments, both the optical end-point position sensor (LED triangle) and the end-point force sensor (flexible "finger" with strain gauge) were mounted on a plate that spans the ends of the two flexible beams. This mounting is not representative of a typical robot-arm mounting in a significant respect: with it, shear of one beam relative to the other produces output signals before either beam tip has actually displaced. (Due to the beam's high flexibility in the horizontal plane but stiffness in the vertical plane, the side rails can slide parallel to each other during bending thus rotating the endplate.)

To make the control results generally useful, it was necessary to repeat the development and demonstrations of Ref. 2 with the two sensors on one of the beams itself. This has now been accomplished. The new arrangement is depicted in Figure II-1 and can be compared to pictures from Ref. 2. By locating the finger on the side rail, we are guaranteed a local reference frame parallel to the beam's center line or neutral axis. The difference in performance for the two arrangements can be seen in the response to step changes in force commands in Figure II-2 of this report. Compare this response to the response in Figure 6 of Ref. 1 and it is evident that the initial anamolous "wiggle" has now been removed. This was alluded to in the note at the bottom of page 16 in Ref. 2.

For subtasks 4.1.1.1 and 4.1.1.2 of the contract work statement, Jim Maples was able to successfully slew and touch to a moving target. This is a tremendous accomplishment in that it incorporates all the system components, control algorithms, and switching algorithms in one demonstration. As Figure 4(a) of Ref. 2 depicts, a model train with a target on it moves away from the arm on an arc of railroad track. Once the train and target are under the hood and in the field of view of the endpoint sensor, the arm begins a rapid large angle slew to chase the train. Contact is made without pause in either the train's or arm's motion while still in the field of view of the optics system, as demonstrated by the experimental time traces of Figure 7, Ref.2. The train and the arm continue to move as the contact force between them is regulated to a commanded level.

The slew-and-touch control is done in three stages with different gains and sensor sets. The theoretical basis for deriving the estimator and controller gains in the Kalman filters will be discussed under Task 4 and in Appendix A.

For the new system, the time response during this same maneuver is given in Figure II-3 (of this report). The commanded force level is achieved after touchdown when the train is both moving and later stopped. The closed loop bandwidth demonstrated is 1.2

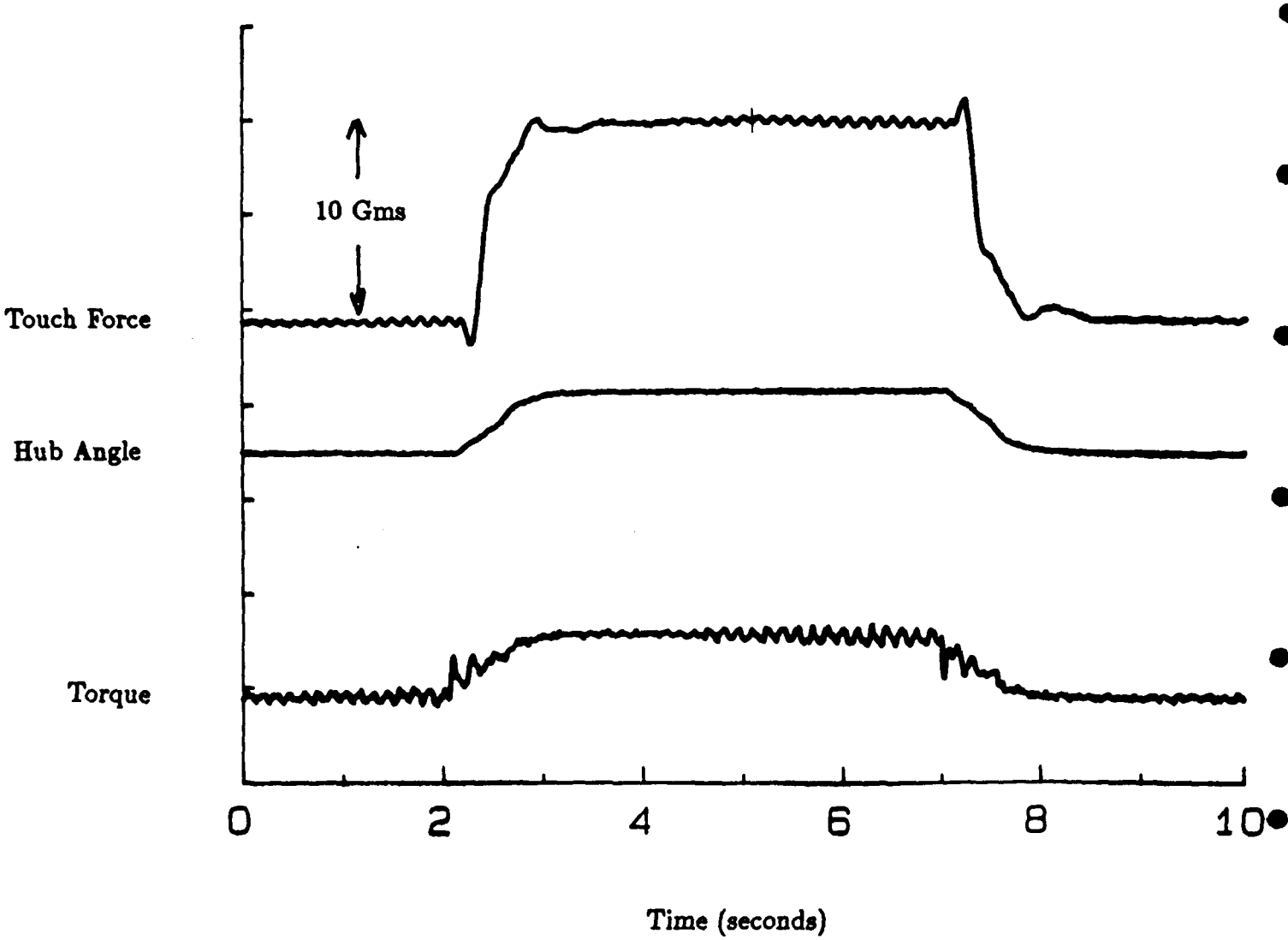

Figure II-2 Step Response – Touch Mode

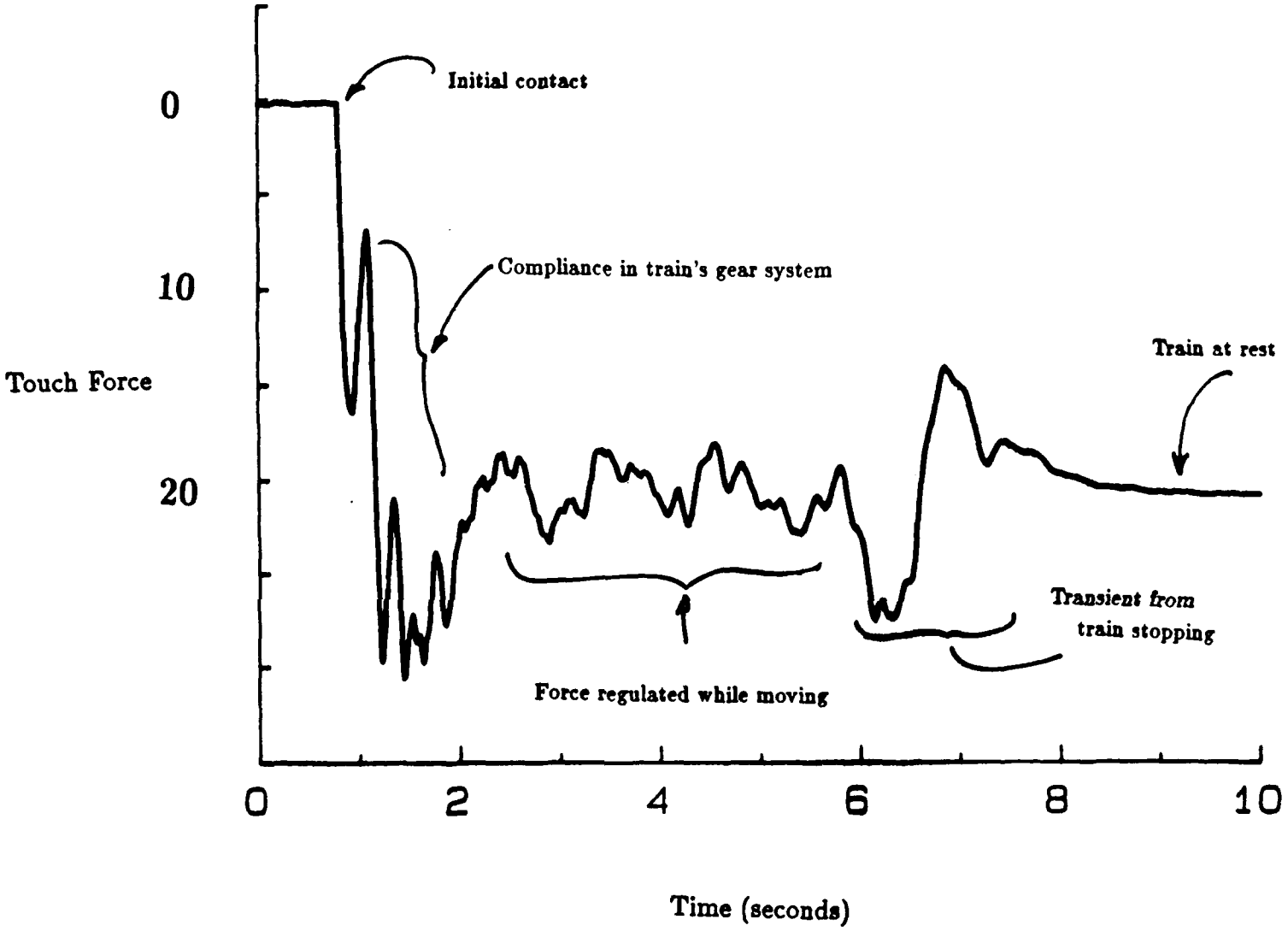

Figure II-3 Touchdown on Moving Train

Hz (faster than the 1 Hz level of the first uncontrolled resonant mode in touch contact). The "noisy" behavior of the signal just after contact comes from the motion of the target (toy railroad car) itself.

During this second year, studies were made of the relation between contact velocities and commanded force levels that have significance in relation to subtasks 4.1.1.3. Force overshoot versus contact velocity is plotted in Figure II-4. The first noticable point is the constancy of the size of the initial force spike for a given velocity. This is to be expected, as it is the impulse reaction of the beam smacking the target and transferring its momentum. Obviously the response appears best when the initial spike and the commanded force level are of comparable size. Worst-case conditions are low-contact-velocity/high-commanded-force and high-contact-velocity/low-commanded-force. In fact, in the low-velocity/high-commanded-force case, the force level command profile should not be a step, but a smoothed spline fit to ease the abrupt transition in force.

Figure II-5 helps one to understand this problem further. If the force level commanded at the moment of contact is the full amount, the controller will detect a large error in desired force level and command a large hub torque. The beam has nonminimum phase characteristics (due to the wave propogation time delay, and the tip will move first away from the target and out of contact. The position controller is now operating to zero the closure distance, and the tip zooms in and smacks the target. The bouncing can be quite violent and unpredictable. This is a very complicated phenomenon involving wave propagation time, nonminimum phase characteristics, and competing control algorithms in position and touch modes. In this case, fairing the command eliminates the bounce; however in the high-velocity/low-force case, a command smoothing will make things worse. Figure II-5 shows this case also. Obviously this important problem demands more investigation for a more generic solution.

Wave propagation speeds have been investigated, and Figure II-6 depicts the associated time lag. The hub moves almost immediately after the command, but the beam tip does not move for about 100 msec. This is the wave propagation time. Also, initially the beam moves the other way, this is the nonminimum phase characteristic. Ultimately the beam tip moves in the desired direction after 290 msec. in position mode (or 250 msec. in touch mode). These are ultimate limits in response time.

For subtask 4.1.1.5, other time delays have been investigated. The motor and sensor response times are essentially instantaneous compared to the beam's bandwidth; however any noise filtering or pseudo-differentiation in the sensors that introduces poles or zeros comparable to the plant's poles must be modeled at the control design stage with auxilliary states.

Digital effects are very important, the most significant being the effective half-sample-period delay introduced in a sample-and-hold digital system. This phase delay is critical in lightly damped systems. In general, the microprocessor must sample at least twice as fast as the highest significant bending mode frequency, and preferably faster.

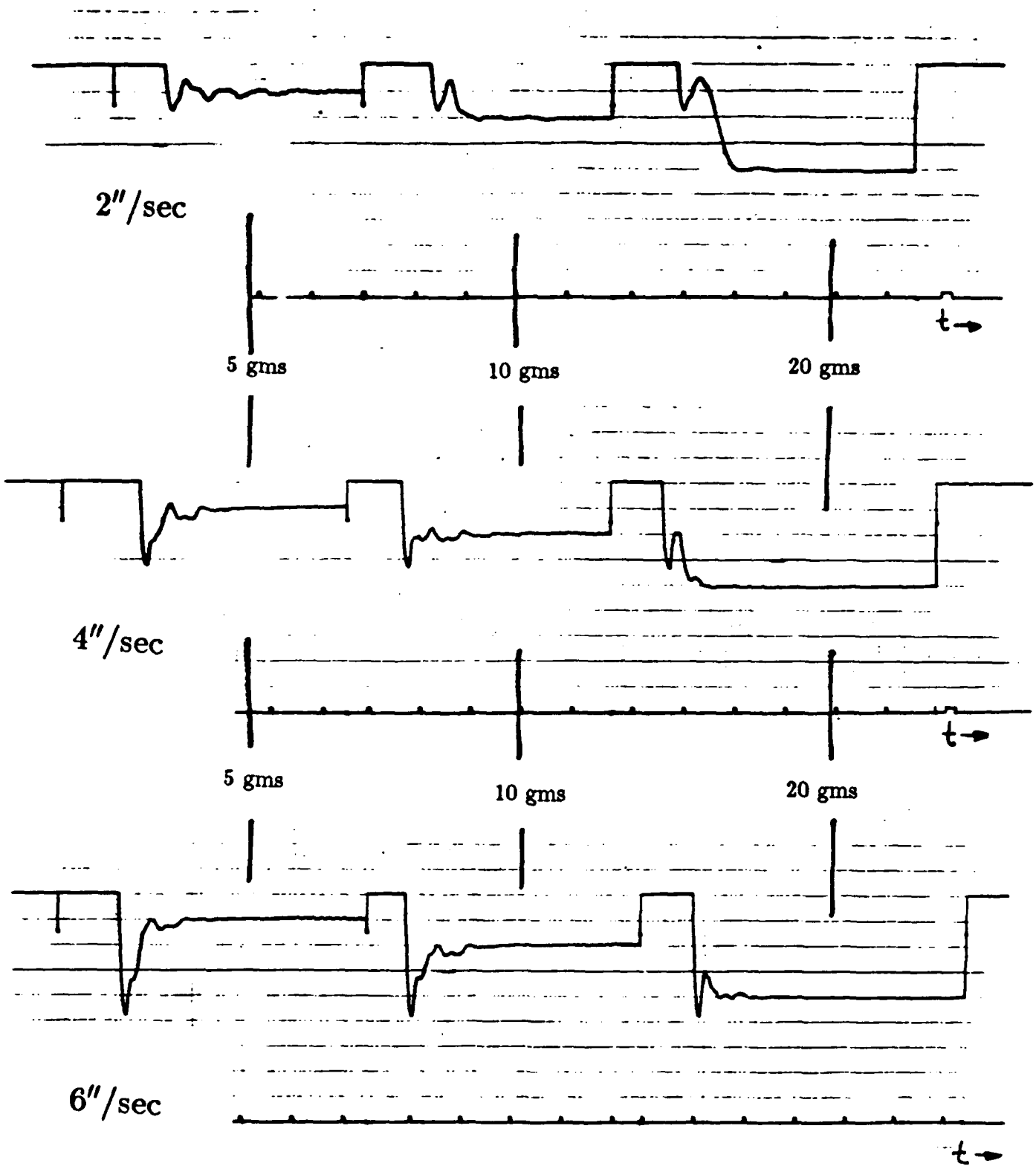

Figure II-4 Force Overshoot Versus Contact Velocity

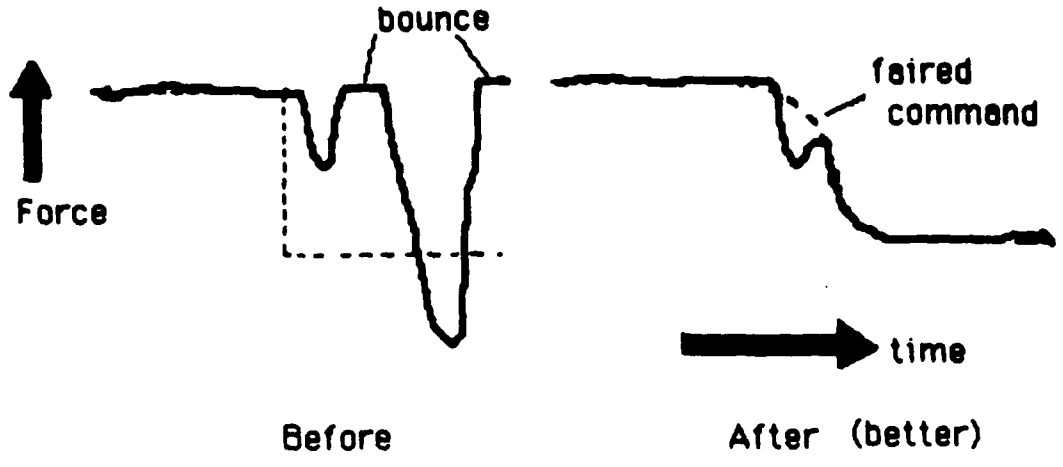

Case 1: Low Contact Velocity/High Force Level Command

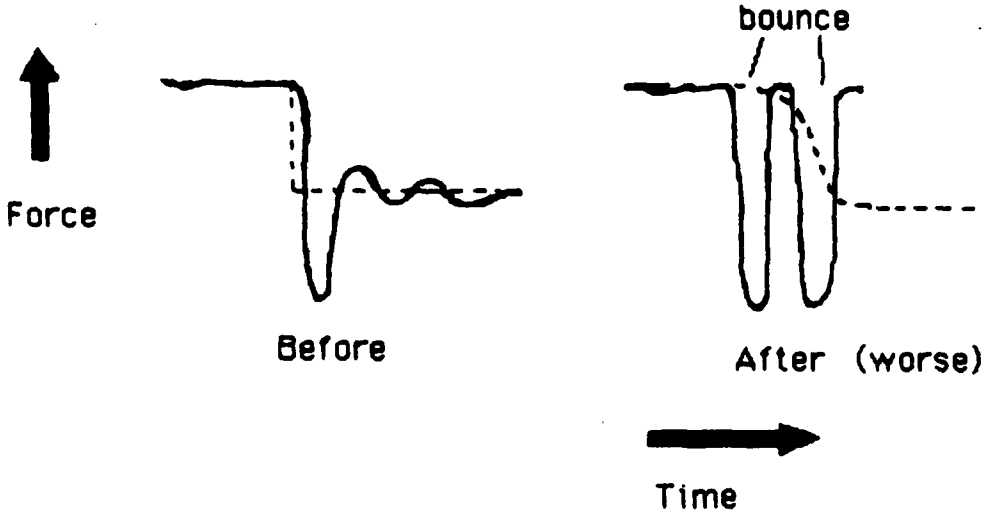

Case 2: High Contact Velocity/Low Force Level Command

Figure II-5 Command Fairing during Touchdown

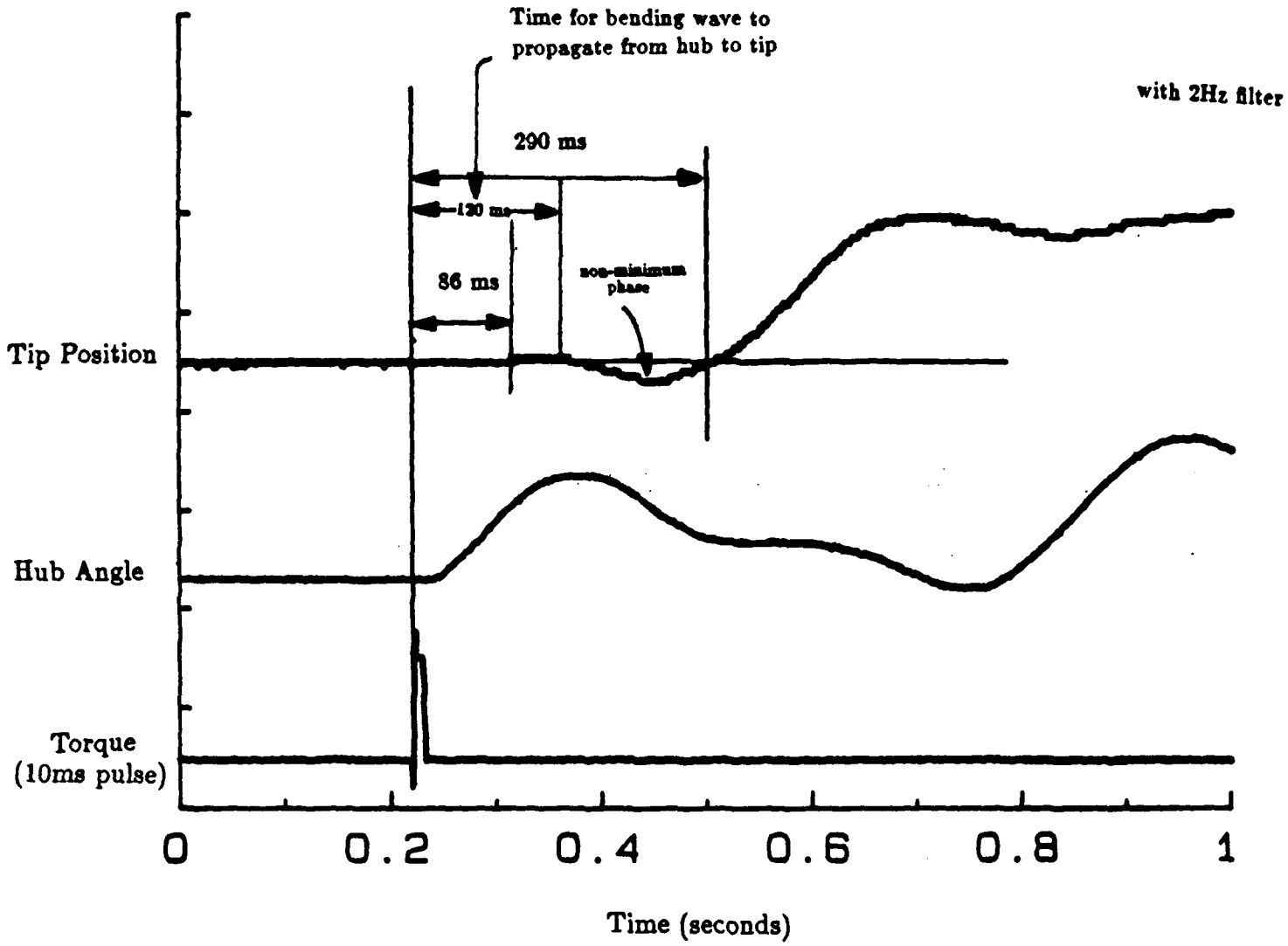

Figure II-6 Wave Propagation – Propagation Mode

Task 2 (4.1.2). Develop Precision End-Point Sensors.

All three subtasks were completed last year (see Ref. 2, p.20).

In relation to 4.1.2.2, (force and proximity sensors), force fingers were successfully used with the flexible beam in touch mode. We have accomplished also an excellent emulation of control with proximity sensors in the following way. Both end-point and target are equipped with LED's and can be clearly distinquished from each other. This is done through time multiplexing. The actual recognition of individual LED's occurs one at a time in a hybrid circuit running at 1KHz external to the microprocessor. The fast response time of the LED's and the optical sensor makes it possible for *one* LED (either target or end point) to be on and sensed every other millisecond. The signal paths in the time multiplexer are synchronized so both analog positions signals are available to the microprocessor for sampling and each position is being updated every other millisecond. Some noise is inherent in this circuit and 10 Hz low pass filters are added on the outputs. These filters each add an additional state for the model of the system. With both target and end point position available, the microprocessor can calculate the separation distance. The controller now attempts to regulate the *closure* (to some small negative number to account for the bending in the force finger). This system performed well in the demonstration. More research is under way to improve the endpoint sensor for higher signal to noise ratio, larger field of view, and the ability to detect multiple LED emitters simultaneously. We shall document the underlying theory.

Task 4 (4.1.4). Develop Control Algorithms.

POSITION		TOUCH
RIGID BODY	----POLE-----	0.99 HZ
0.49 HZ	----ZERO-----	1.39 HZ
1.78 HZ	----POLE-----	2.35 HZ
2.60 HZ	----ZERO-----	3.24 HZ
3.28 HZ	----POLE-----	3.64 HZ
7.01 HZ	----ZERO-----	7.22 HZ
7.21 HZ	----POLE-----	7.52 HZ *

*Amplitude dependent

Figure II-7 Chart of Resonant Frequencies

The development of sophisticated control and switching algoritms (subtask 4.1.4.1) is a very complicated process, but there are basic guidelines followed in the control design procedure. The starting point in controlling a plant is always understanding and modeling its dynamics. The flexible beam has dynamics that are different for the position and for the touch mode because of changing boundary conditions. The beam essentially is pinned at the hub and free at the tip in this position mode, but pinned at both ends in touch.

The corresponding resonant frequencies, obtained through sine sweep techniques, are very different as shown in Figure II-7. (These are for the colocated transfer function of the hub angle to torque control. The alternating pole-zero sequence on the $j\omega$-axis is typical of colocated sensors and actuators, and feedback will always guarantee a stable, but slow, closed-loop system.) By using feedback instead from position or force at the ***end*** of the flexible beam, the colocation of sensors and actuators is relinquished. The corresponding non-colocated transfer functions now contain right-half-plane zeros which are certain to drive the controller unstable unless either very low gains are used (basically open loop) or the plant's dynamics between the actuator and endpoint are well modeled and used as the basis for very sophisticated control. However, sensing directly the quantity to be controlled (end point position or force) pays off handsomely, not only in high precision, but in much faster speed of response and much greater disturbance rejection (typically an order of magnitude). Achieving this difficult kind of control is the focus of our research.

Using these transfer functions and the residues of each resonant mode at each sensor, it is possible to derive a state space representation of the plant in the following form:

$$\dot{x} = Fx + Gu \qquad \text{x = state vector}$$

$$\text{u=control output}$$

$$y = Hx \qquad \text{y = sensor measurements}$$

The exact form of these matrices is detailed in Appendix A and a generalized discussion of them may be found in Ref. 3. For an optimal controller, a penalty function J is defined as follows:

$$J = \text{integral } x\,Ax + u\,Bu \qquad \text{A = penalty on states}$$

$$\text{B = penalty on control}$$

In this case, we are controlling tip position or tip force, the quantities being measured. Taking the appropriate row vector from H and calling it H', the desired quantity at the endpoint can be penalized by forming A such that:

$$y' = H'x \qquad y\,y = x\,H\,Hx \qquad A = H\,H$$

In a single-input single-output system, the relative size of A and B is most important in the optimal control algorithms. To find constant control gains, a matrix Riccati equation is solved which can be thought of in terms of a symmetric root locus varying with A/B. Here, many sensors are used and, in the future, more than one actuator may be used; so the relative sizes of internal elements of A and B are important. The optimal control algorithms to determine gains are incorporated in various computer codes, such as Stanford's OPTSYS (for continuous systems) and DISC (for discretized systems),and this step is done iteratively until the closed-loop eigenvalues are at more desirable locations. This gives full state feedback of the form:

$$u = -Cx$$

The states x, however, are not all obtained directly and must be estimated from the sensors. The estimator gains are obtained in a similar manner to the control gains: by modeling error equations and accounting for noise and uncertainty in the measurements. These principles for optimal control and Kalman filtering are well documented in Ref. 4 and discussed in more detail in Appendix A.

These techniques have worked well for linear systems; but the flexible beam has nonlinearities and therefore another pass through the design iteration procedure is required and discussed in Task 6 under functional assessment. The above-mentioned gains were derived for particular tasks, and the three tasks required for the slew and touch to a moving target are:

1. Large-angle slew — Beam configuration: pinned-free. Sensors used: hub angle and rate, strain rate.
2. Closure to target — Beam configuration: pinned-free. Sensors used: optical tip position, hub rate, strain rate.
3. Touch — Beam configuration: pinned-pinned. Sensors used: tip force, hub rate, strain rate.

The switching between the three sets of estimator and control gains is done smoothly by initializing the estimator states to zero at the moment of switching to the new gains. The start-up transients are small and die out quickly enough to justify this simplistic approach. More complicated switching initialization techniques to insure continuous state throughout were found to improve performance only slightly at the expense of more complexity and calculation time. This is a very important result, which we will document more generically during the coming year. In particular, one exception will occur when going from touch to position, where the rigid body modes have to be initialized at the proper position. This has not been part of the slew and touch demonstrations to date.

Task 6 (4.1.6). Make Functional Assessment

After applying the controller derived for the linear model to the flexible beam, problems in touch were addressed and solved as required in subtask 4.1.6.2. The command fairing problem was discussed in Task 1. The control in touch needs an integral component to respond well, because the steady state error will be large without it. The difficulty in implementing the integral control was solely in setting up the modeled equations and running it in the DISC software.

Another problem detected involved a nonlinearity, the amplitude dependence of the fourth mode's resonant frequency. The resonant frequency would vary from 8.8 Hz at low input amplitudes to 7.5 Hz at high input amplitudes. The plant controller was designed with the frequency at 7.5 Hz to insure that large-amplitude responses would be controlled. This results in a low-amplitude buzzing with high frequency, slowly growing in amplitude until its frequency shifts low enough to be notched out by the controller. This is seen as the small buzzing in Figure 2, the step response in touch. Another attempt to reduce the

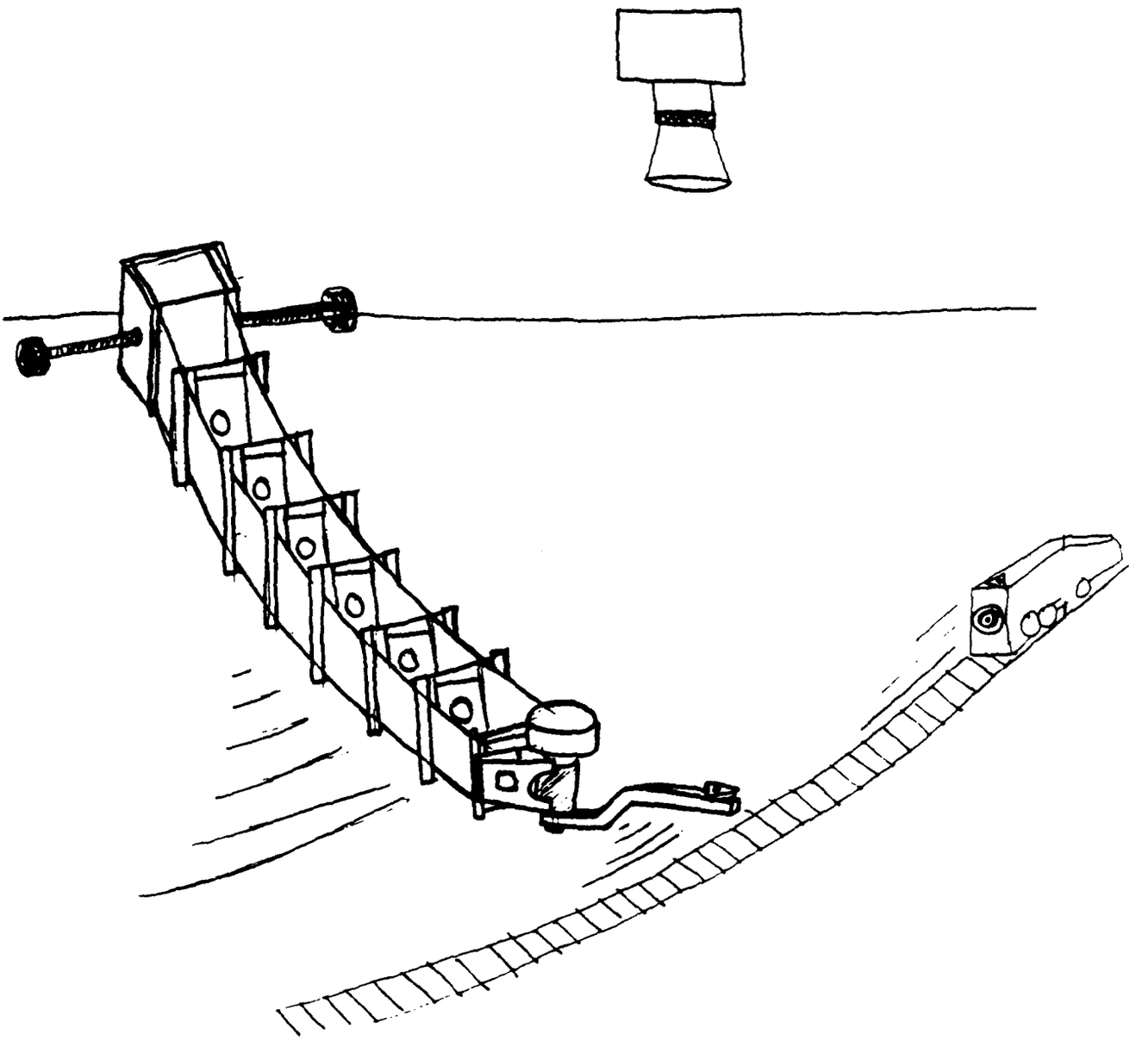

Figure II-8 New Flexible Arm with Fast Wrist

effects of these higher modes and nonlinearities is the addition of a 2 Hz low-pass filter on the control output. This works well and, as suggested in Ref. 5, it is possible to put filters on the outputs with bandwidths as low as the desired closed-loop bandwidth of the system.

More improvements are possible, especially in the area of model order reduction. The present controller runs with 12 states, making matrix operations cumbersome. Using new algorithms developed at Stanford (gradient search methods such as in SANDY code), it will be possible to ascertain which states are more critical in control and reduce the model order. Preliminary results on a flexible beam in position mode have shown it to perform well with a fourth order controller and similarly to an eighth order controller.

FUTURE PLANS

Task 3 (4.1.3). New Designs — Flexible Arm with Rigid, Fast Wrist and Two-Link Arm

Preliminary research in position control has shown that much better system performance, notably in bandwidth and in slew and snatch maneuvers, can be obtained for a flexible arm and rigid wrist than with a single flexible arm. In addition, very fast response is posssible in a localized region. We expect to reap this same benefit for touch control also, and especially for slew-and-touch; and we have begun work in this DARPA program to so demonstrate.

Figure II-8 shows a new flexible arm with a wrist that has been constructed and is being instrumented. Higher closed loop bandwidth in touch is expected. This system has multiple inputs and outputs making control more complicated but much more useful in real world applications. This system is also being equipped to sense multiple targets simultaneously and may incorporate a load cell to sense force rather than a force finger with its associated compliance. Initial experiments will include another demonstration of the slew and touch to the moving model train.

Also in Year 3 we plan to develop force control and slew-and-touch capability for the two-link-arm with flexible tendons that was designed and built last year with joint DARPA-AFOSR funding, and for which we are currently developing basic end-point optical control algorithms under AFOSR funding.

References

1. DARPA Contract #F33615-82-K-5108, September, 1982.
2. Binford, T.O., Cannon, R.H. *"First Annual Report on End Point Control of Flexible Robots."* Aeronautics and Astronautics Dept., Stanford University, May 1984.
3. Cannon, R.H., Schmitz, E., *"Initial Experiments on the End-Point Control of a Flexible One Link Robot,"* Submitted to the Journal of Robotics, December 1983.
4. Bryson, A.E., and Ho, Y.C., *"Applied Optimal Control,"* John Wiley and Sons, New York, 1969.
5. Franklin, G., and Powell, D., *"Digitial Control of Dynamic Systems,"* Addison Wesley, 1984.

Appendix A
DERIVATON OF CONTROLLER AND ESTIMATOR GAINS

The resonant frequencies of the flexible beam are determined in sine sweep tests by monitoring the torque input and the sensor output on an oscilloscope. With lightly damped poles, the local maxima in the output are easily identified. If the poles are also well separated on the $j\omega$-axis, the output of the driven system is mainly the residue of that natural frequency with little contribution from the other modes. The beam theoretically has an infinite number of resonant frequencies, but non-linear effects begin to dominate above 10 Hz. By choosing a particular sensor, the peak to peak output measured is the numerator (residue) of a mode for that particular transfer function at that mode. Modal analysis is a direct way to attain a state space representation of the beam as shown in Figure A1.

The parallel paths of U(s) are the equivalent of a partial fraction expansion of the transfer function between sensor and actuator. Each sensor has a particular set of modal residues (the H's) associated with it. The states developed are q_i and $\dot{q}_i$ for each mode. To obtain an open loop pole-zero plot, the zeros of the colocated sensor-actuator transfer function may be identified on the oscilloscope as local minima (this is possible as the zeros are guaranteed to lie on the $j\omega$-axis between the poles). The noncolocated case is more difficult as the partial fraction expansion must be combined and the numerator factored to find the zeros. Their locations are severly affected by the truncation of the infinite series of resonances and the numerical accuracy with which the residues were recorded. However, the non-minimal characteristics are still evident as seen in comparing Figure A2 and Figure A3. It can be seen that a noncolocated sensor-actuator system with feedback will normally go unstable unless something special is done.

Optimal control techniques are useful, since many inputs and/or outputs are being considered at once. Successive loop closure and root locus techniques are also useful to lend direct physical significance; but they may entail more lengthy analysis, as many parameters are free to vary at once. The F matrix was described in Figure A1, and the H matrix is composed of residues of each mode for each sensor. The G matrix is comprised of alternating 1's and 0's, as the scale factor has already been absorbed into the the H matrix. Figure A4 depicts the closed-loop system in touch mode and the numerical values of the basic F, G, and H matrices. In position control mode, the plant model would include a rigid-body mode in place of the first resonant mode.

The final F, G, and H matrices are not yet complete. For some sensors, it is desirable to decrease noise by putting a 10 Hz filter on the outputs. This extra dynamic relation is accounted for by augmenting the matrices with auxilliary states. The same concept applies for pseudo-differentiators, integral control, and the 2 Hz filter on the motor control output. The model for four resonant modes, which has now grown from 8th order to 12th order, is now ready for control and estimator gain calculations.

In touch mode, contact force is being regulated so the A penalty matrix is formed from the row of H associated with the force sensing finger. The value of A is given below without the additional filter states (hence an 8 x 8 matrix).

$$H' = [\,240.6 \quad 0 \quad -933.5 \quad 0 \quad 888.7 \quad 0 \quad -644.2 \quad 0\,]$$

$$A = H'H'/1000 = \begin{bmatrix} 57.89 & 0 & -224.6 & 0 & 213.8 & 0 & -155.0 & 0 \\ 0 & 0^* & 0 & 0 & 0 & 0 & 0 & 0 \\ -224.6 & 0 & 871.4 & 0 & -829.6 & 0 & 601.4 & 0 \\ 0 & 0 & 0 & 0^* & 0 & 0 & 0 & 0 \\ 213.8 & 0 & -829.6 & 0 & 789.8 & 0 & -572.5 & 0 \\ 0 & 0 & 0 & 0 & 0 & 0^* & 0 & 0 \\ -155.0 & 0 & 601.4 & 0 & -572.5 & 0 & 415.0 & 0 \\ 0 & 0 & 0 & 0 & 0 & 0 & 0 & 0^* \end{bmatrix}$$

With a single actuator, the control penalty B is a scalar and can be varied to give different values of A/B. This ratio of penalties on states and control effort drives the algorithm internal to DISC to yield closed loop eigenvalues. Also the zero diagonal terms (starred) in A may be adjusted to put penalties on velocities $\dot{q}_i$, thereby adding damping. After adjusting the relative weightings in A and B, suitable closed loop eigenvalues are quickly determined.

The program DISC will take continuous time matrices for plant dynamics, measurements, control distribution, and penalty functions and then discretize them according to the specified sample rate running the digital controller. The constant control gains are calculated from the steady state, discrete, matrix Riccati equation. At the same time, noise covariances for process and sensor noise are specified for generating estimator gains. The noise was assumed to be Gaussian and its levels in the A/D, sensors, and other electronics was measured. It is extremely important to note that the addition of an endpoint sensor to measure a quantity at the tip (that is to be controlled) speeds up the estimator immensely. The response of the estimator in tracking the states is critical to the closed loop performance of the system.

The last part of the appendix includes printouts of computer runs on DISC to generate controller and estimator gains. Both are in position mode, but one uses the endpoint sensor and has its slowest estimator pole at 1.17 Hz while the other run uses no endpoint sensing and has its slowest estimator pole at .37 Hz. Also note the change in the matrix forms from the basic form shown in Figure A4.

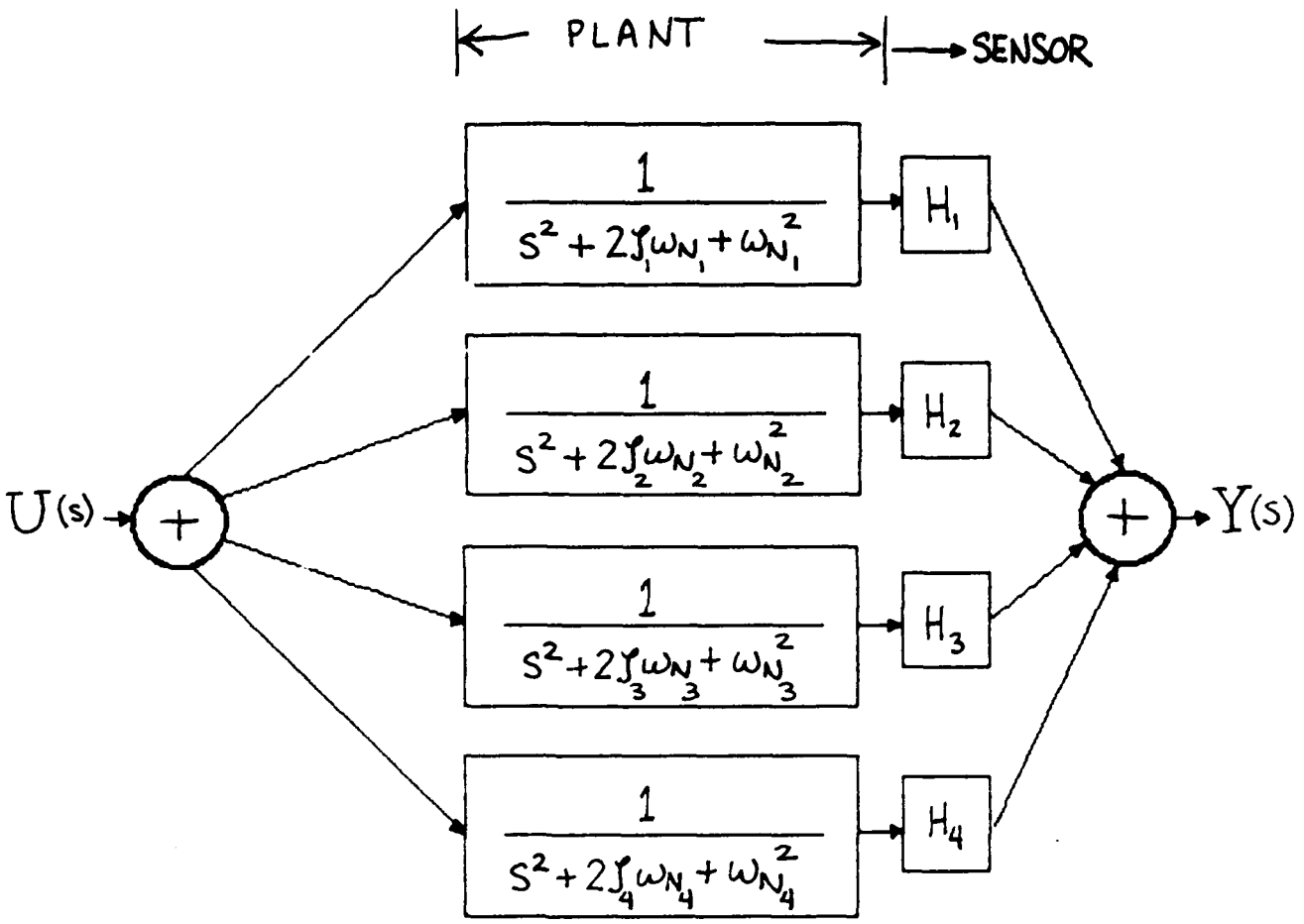

Modal Form for Beam

$$F = \begin{bmatrix} \begin{bmatrix} 0 & 1 \\ -\omega_{N_1}^2 & -2\zeta_1\omega_{N_1} \end{bmatrix} & & & \\ & \begin{bmatrix} 0 & 1 \\ -\omega_{N_2}^2 & -2\zeta_2\omega_{N_2} \end{bmatrix} & & \\ & & \begin{bmatrix} 0 & 1 \\ -\omega_{N_3}^2 & -2\zeta_3\omega_{N_3} \end{bmatrix} & \\ & & & \begin{bmatrix} 0 & 1 \\ -\omega_{N_4}^2 & -2\zeta_4\omega_{N_4} \end{bmatrix} \end{bmatrix}$$

Figure A1

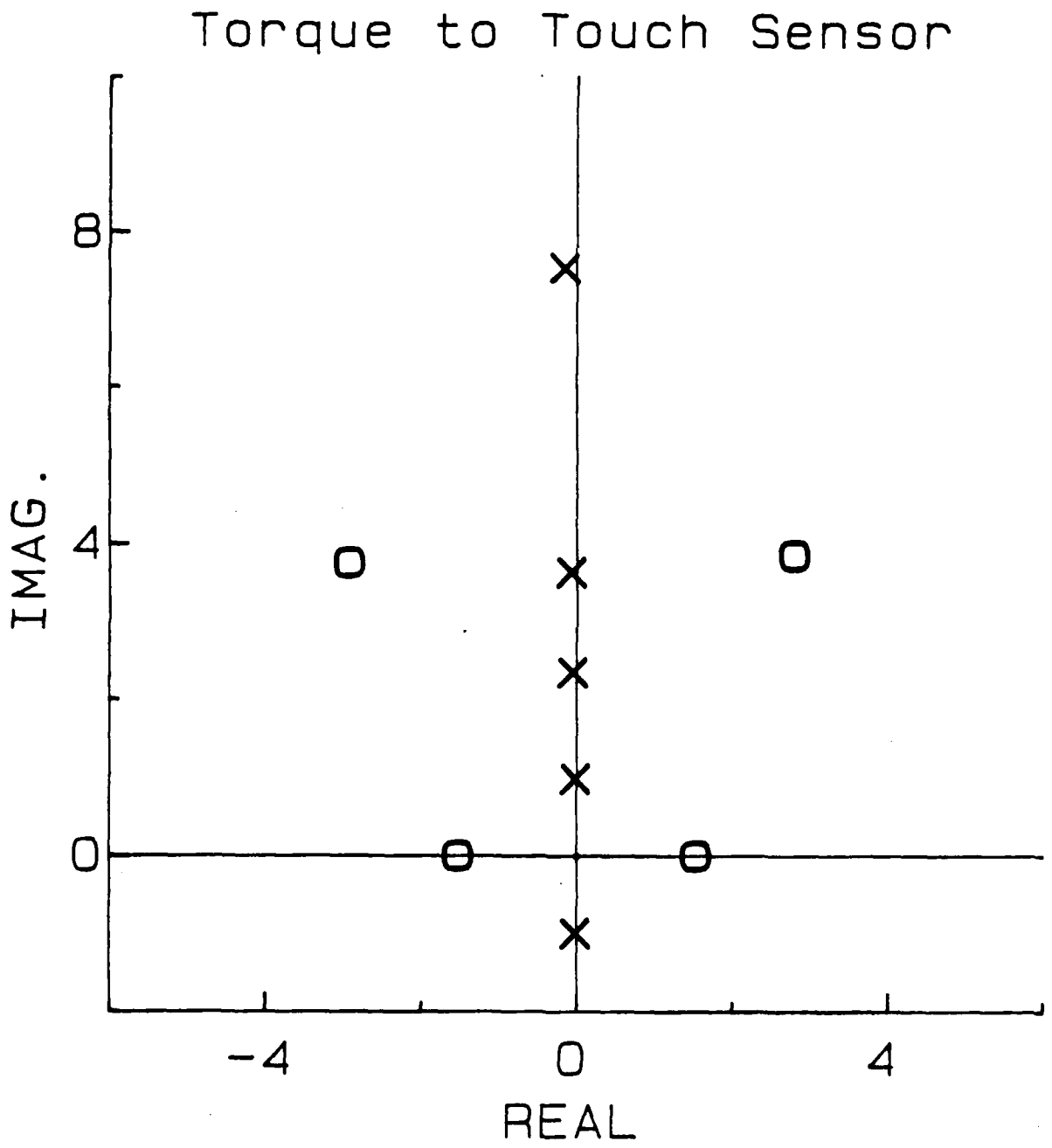

Figure A2

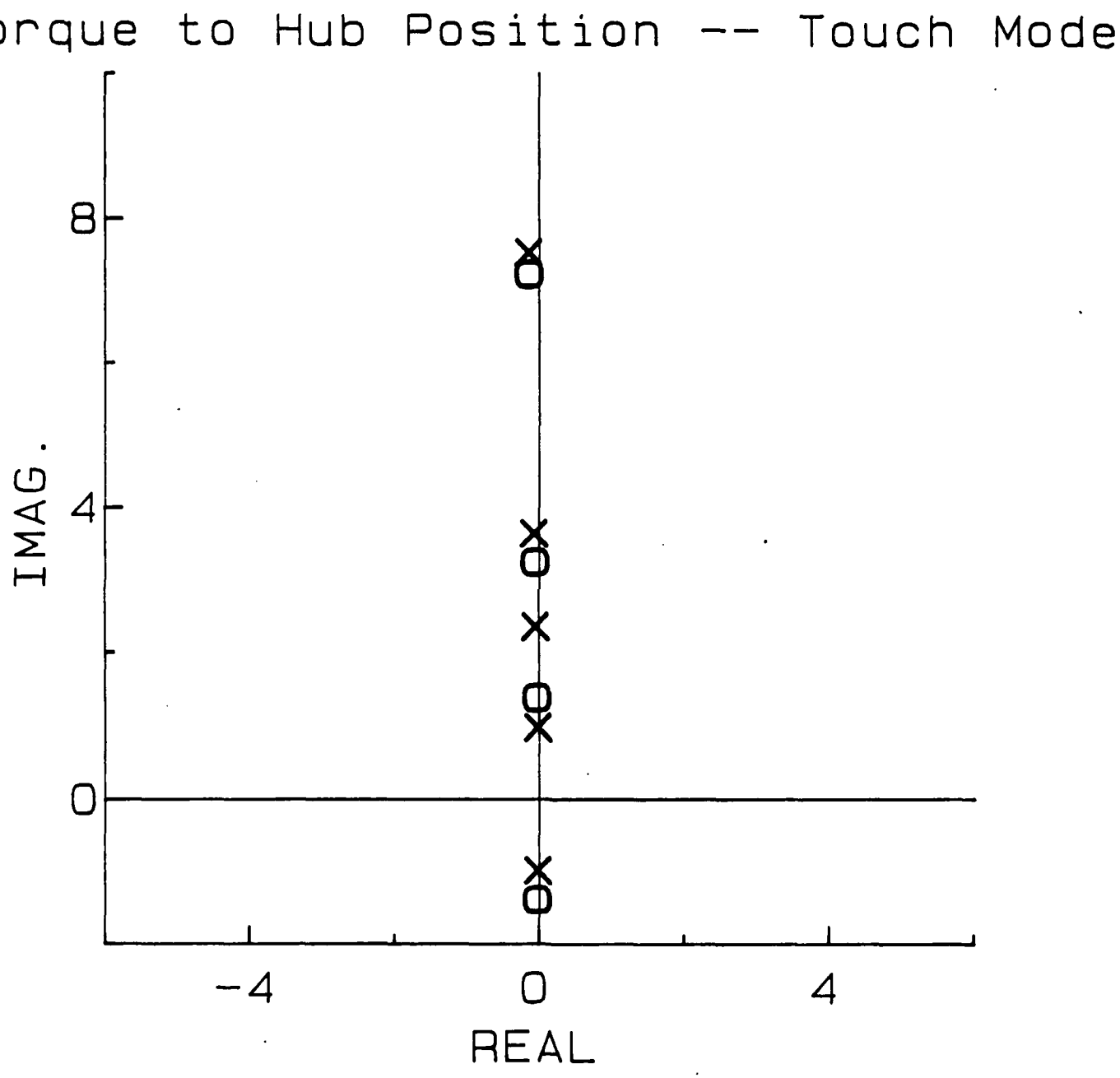

Figure A3

FORCE CONTROL

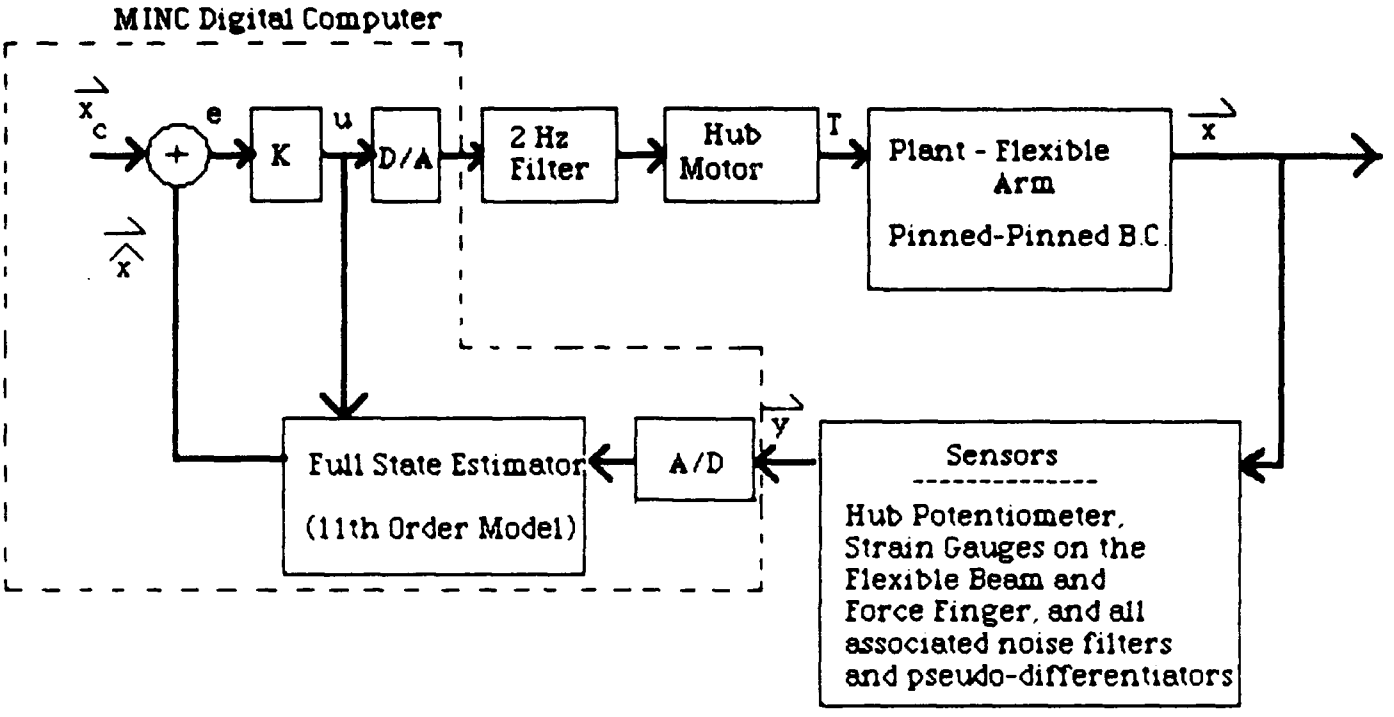

$$\frac{d}{dt}\begin{bmatrix} q_1 \\ \dot{q}_1 \\ q_2 \\ \dot{q}_2 \\ q_3 \\ \dot{q}_3 \\ q_4 \\ \dot{q}_4 \end{bmatrix} \equiv \begin{bmatrix} 0 & 1 & & & & & & \\ -38.4 & -.248 & & & & & & \\ & & 0 & 1 & & & & \\ & & -218.0 & -.591 & & & & \\ & & & & 0 & 1 & & \\ & & & & -523.1 & -.915 & & \\ & & & & & & 0 & 1 \\ & & & & & & -2232.5 & -1.89 \end{bmatrix} \begin{bmatrix} q_1 \\ \dot{q}_1 \\ q_2 \\ \dot{q}_2 \\ q_3 \\ \dot{q}_3 \\ q_4 \\ \dot{q}_4 \end{bmatrix} + \begin{bmatrix} 0 \\ 1 \\ 0 \\ 1 \\ 0 \\ 1 \\ 0 \\ 1 \end{bmatrix} u$$

$$\begin{bmatrix} \theta \\ SG \\ Y \end{bmatrix} \equiv \begin{bmatrix} 5.43 & 0 & 16.73 & 0 & 10.63 & 0 & 3.27 & 0 \\ 10.21 & 0 & 35.80 & 0 & -46.77 & 0 & -73.25 & 0 \\ 240.6 & 0 & -933.5 & 0 & 888.7 & 0 & -644.2 & 0 \end{bmatrix} \begin{bmatrix} q_1 \\ \vdots \\ \dot{q}_4 \end{bmatrix}$$

$\dot{\vec{x}} = F\vec{x} + Gu$ $\quad q_i = \text{position}_i$

$\vec{y} = H\vec{x}$ $\quad \dot{q}_i = \text{velocity}_i$

Figure A4